21. Valdiglesias V, Giunta S, Fenech M, Neri M, Bonassi S (2013) gammaH2AX as a marker of DNA double strand breaks and genomic instability in human population studies. Mutat Res 753: 24–40.
22. Ohashi S, Natsuizaka M, Naganuma S, Kagawa S, Kimura S, et al. (2011) A NOTCH3-mediated squamous cell differentiation program limits expansion of EMT-competent cells that express the ZEB transcription factors. Cancer Res 71: 6836–6847.
23. Toda Y, Kono K, Abiru H, Kokuryo K, Endo M, et al. (1999) Application of tyramide signal amplification system to immunohistochemistry: a potent method to localize antigens that are not detectable by ordinary method. Pathol Int 49: 479–483.
24. Tajima Y, Nakanishi Y, Ochiai A, Tachimori Y, Kato H, et al. (2000) Histopathologic findings predicting lymph node metastasis and prognosis of patients with superficial esophageal carcinoma: analysis of 240 surgically resected tumors. Cancer 88: 1285–1293.
25. Nozoe T, Oyama T, Takenoyama M, Hanagiri T, Sugio K, et al. (2006) Significance of immunohistochemical expression of p27 and involucrin as the marker of cellular differentiation of squamous cell carcinoma of the esophagus. Oncology 71: 402–410.
26. McMahon KS, Wieman TJ, Moore PH, Fingar VH (1994) Effects of photodynamic therapy using mono-L-aspartyl chlorin e6 on vessel constriction, vessel leakage, and tumor response. Cancer Res 54: 5374–5379.
27. Luna MC, Ferrario A, Wong S, Fisher AM, Gomer CJ (2000) Photodynamic therapy-mediated oxidative stress as a molecular switch for the temporal expression of genes ligated to the human heat shock promoter. Cancer Res 60: 1637–1644.
28. Evans HH, Horng MF, Ricanati M, Deahl JT, Oleinick NL (1997) Mutagenicity of photodynamic therapy as compared to UVC and ionizing radiation in human and murine lymphoblast cell lines. Photochem Photobiol 66: 690–696.
29. Calaf G, Russo J (1993) Transformation of human breast epithelial cells by chemical carcinogens. Carcinogenesis 14: 483–492.
30. McCormick JJ, Fry DG, Hurlin PJ, Morgan TL, Wilson DM, et al. (1990) Malignant transformation of human fibroblasts by oncogene transfection or carcinogen treatment. Prog Clin Biol Res 340D: 195–205.
31. Taparowsky EJ, Heaney ML, Parsons JT (1987) Oncogene-mediated multistep transformation of C3H10T1/2 cells. Cancer Res 47: 4125–4129.
32. Liu L, Zhang Z, Xing D (2011) Cell death via mitochondrial apoptotic pathway due to activation of Bax by lysosomal photodamage. Free Radic Biol Med 51: 53–68.
33. Miki Y, Akimoto J, Yokoyama S, Homma T, Tsutsumi M, et al. (2013) Photodynamic therapy in combination with talaporfin sodium induces mitochondrial apoptotic cell death accompanied with necrosis in glioma cells. Biol Pharm Bull 36: 215–221.
34. Saito K, Mikuniya N, Aizawa K (2000) Effects of photodynamic therapy using mono-L-aspartyl chlorin e6 on vessels and its contribution to the antitumor effect. Jpn J Cancer Res 91: 560–565.

Huang et al. Journal of Biomedical Science 2014, 21:44
http://www.jbiomedsci.com/content/21/1/44

科技部 Ministry of Science and Technology
The cost of publication in Journal of Biomedical Science is borne by the Ministry of Science and Technology, Taiwan.

JBS JOURNAL OF BIOMEDICAL SCIENCE

RESEARCH Open Access

Prospective signs of cleidocranial dysplasia in Cebpb deficiency

Boyen Huang[1,2], Katsu Takahashi[2*], Ernest A Jennings[1], Pongthorn Pumtang-on[3], Honoka Kiso[2], Yumiko Togo[2], Kazuyuki Saito[2], Manabu Sugai[4], Shizuo Akira[5], Akira Shimizu[4] and Kazuhisa Bessho[2]

Abstract

Background: Although runt-related transcription factor 2 (RUNX2) has been considered a determinant of cleidocranial dysplasia (CCD), some CCD patients were free of RUNX2 mutations. CCAAT/enhancer-binding protein beta (Cebpb) is a key factor of Runx2 expression and our previous study has reported two CCD signs including hyperdontia and elongated coronoid process of the mandible in Cebpb deficient mice. Following that, this work aimed to conduct a case-control study of thoracic, zygomatic and masticatory muscular morphology to propose an association between musculoskeletal phenotypes and deficiency of Cebpb, using a sample of $Cebpb^{-/-}$, $Cebpb^{+/-}$ and $Cebpb^{+/+}$ adult mice. Somatic skeletons and skulls of mice were inspected with soft x-rays and micro-computed tomography (μCT), respectively. Zygomatic inclination was assessed using methods of coordinate geometry and trigonometric function on anatomic landmarks identified with μCT. Masseter and temporal muscles were collected and weighed. Expression of Cebpb was examined with a reverse transcriptase polymerase chain reaction (RT-PCR) technique.

Results: $Cebpb^{-/-}$ mice displayed hypoplastic clavicles, a narrow thoracic cage, and a downward tilted zygomatic arch ($p < 0.001$). Although $Cebpb^{+/-}$ mice did not show the phenotypes above ($p = 0.357$), a larger mass percentage of temporal muscles over masseter muscles was seen in $Cebpb^{+/-}$ littermates ($p = 0.012$). The mRNA expression of Cebpb was detected in the clavicle, the zygoma, the temporal muscle and the masseter muscle, respectively.

Conclusions: Prospective signs of CCD were identified in mice with Cebpb deficiency. These could provide an additional aetiological factor of CCD. Succeeding investigation into interactions among Cebpb, Runx2 and musculoskeletal development is indicated.

Keywords: Cebpb, Cleidocranial dysplasia, Clavicle, Thoracic cage, Zygomatic arch, Masseter, Temporal muscle

Background

Cleidocranial dysplasia (CCD) is a congenital skeletal disease typically manifesting cranial deformity, clavicle hypoplasia and unerupted supernumerary teeth [1-5]. Some human CCD cases also displayed hypotrophy of the masseter muscle, abnormality of the mandible and/or deformation of the zygomatic arch [3-5]. Haploinsufficiency of the runt-related transcription factor 2 (RUNX2 in humans, Runx2 in mice) has been considered a determinant of CCD in humans [6]. A recent study has also identified bony and dental defects consistent with signs of human CCD amongst mice with impaired activity of the Runx2 P1 promoter [7]. Expression of the Runx2 P1 promoter in the developing skull has been confirmed [8] and its activity is essential to establishing a sufficient number of osteoprogenitor cells for normal skeletogenesis [7]. Although the mechanism of CCD-related dental anomalies is not clear, induction of the dentition was associated with fibroblast growth factor (FGF) signaling [9] that was mediated by Runx2 during development of teeth [10] and bone [11]. Nevertheless, about one-third of CCD patients were free of RUNX2 mutations [6]. Furthermore, diverse dental manifestations resulting from identical mutations of the RUNX2 gene have been observed [1]. These infer potential involvement of other factors on occurrence of CCD.

CCAAT/enhancer binding protein beta (CEBPB in humans, Cebpb in mice) is a transcription factor which

* Correspondence: takahask@kuhp.kyoto-u.ac.jp
[2]Department of Oral and Maxillofacial Surgery, Graduate School of Medicine, Kyoto University, Shogoin-Kawahara-cho 54, Sakyo-ku, Kyoto 606-8507, Japan
Full list of author information is available at the end of the article

binds to consensus sequences and affects the transcription of various genes involved in proliferation and differentiation, and found in the liver [12], the mammary gland [13] and the immune system [14,15]. In addition to its relevance in tumorigenesis [16] and adipogenesis [17], previous studies have suggested that Cebpb is a key factor of Runx2 expression in bone formation [18-21]. A reduction in Runx2 expression was accompanied by a decrease in osteogenic potential and shown to be related to ectopic expression of Cebpb [18]. On the other hand, a functional synergism of Runx2 and Cebpb during osteoblast [21] and chondrocyte differentiation [20] has been reported. Suppressed differentiation of osteoblasts and delayed chondrocyte hypertrophy due to a complete deletion of Cebpb is likely to postpone bone formation [19]. This concurs with phenotypes of p20Cebpb (a dominant negative inhibitor of Cebpb) overexpressing mice, including a reduced amount of alveolar bone and a lower bone volume fraction of the mandible [22].

Recent studies have identified multiple supernumerary teeth [23], hypoplastic clavicles [20], an open fontanelle [20] and an elongated coronoid process [23] in mice with Cebpb deficiency. These phenotypes coincide with signs of CCD in humans [1-5] and consequently a relationship between CEBPB and CCD is suspected [20]. To explore prospective signs of human CCD in a murine model, this study aimed to conduct a case-control study of thoracic, craniofacial and myological variations, using a sample of $Cebpb^{-/-}$, $Cebpb^{+/-}$ and $Cebpb^{+/+}$ mice. A special interest was to investigate morphology of the zygomatic arch and mass of both masseter and temporal muscles.

Methods

An appropriate ethics approval has been obtained from the Institutional Review Board of Kyoto University (Reference Number: Med Kyo 11518). $Cebpb^{+/-}$ and $Cebpb^{-/-}$ mice were generated as described previously [15]. Thirty-five adult mice were euthanised with carbon dioxide gas for inspection, including 5 $Cebpb^{-/-}$ (5 female), 16 $Cebpb^{+/-}$ (10 female and 6 male) and 14 $Cebpb^{+/+}$ (8 female and 6 male) mice. All female mice were sacrificed at the age of 12 months, whilst the age of male mice used ranged from 4.5 to 13 months. Owing to a high neonatal mortality of $Cebpb^{-/-}$ mice [24], male animals of this genotype were not attainable in this sample.

Firstly, skeletons of the female mice were imaged with soft x-rays (SOFRON; SRO-M50, Sofron X-ray Industry Corporation Ltd., Tokyo, Japan). Both lateral and dorsal-ventral radiographs of the experimental animals were evaluated by a single-blinded examiner who is a qualified veterinarian.

Secondly, murine skulls of the 23 female mice were assessed with a micro-computed tomography (μCT) scanner (SMX-100CT-SV3; Shimadzu, Kyoto, Japan). This technique was applied to identify predetermined craniofacial landmarks including Landmark LO, LP, RP, LJ, LZ, and LS (Table 1) [23,25,26]. As the external auditory meatus of mice is located at a lower level than that of humans [27], Landmark LP and RP situated slightly superior to the external auditory meatus were used to replace human Porions (the most superior point of external auditory meatus visible on a lateral cephalometric radiograph) to establish a horizontal plane (H plane) with Landmark LO in this study. Following this, a jugal plane (J plane: defined by Landmark LJ, LP, and RP), a zygomatic plane (Z plane: defined by Landmark LZ, LP and RP), and a squamosal plane (S plane: defined by Landmark LS, LP and RP) were established (Figure 1). Usage of the dihedral angles in the assessment of human zygomatic anatomy has been reported [26]. The dihedral angles between H plane and J plane, between H plane and Z plane, and between H plane and S plane were calculated using a method of coordinate geometry and trigonometric function [28]. The following formulae were used.

Given the equation of H plane containing Landmark LO (x_{LO}, y_{LO}, z_{LO}), LP (x_{LP}, y_{LP}, z_{LP}) and RP (x_{RP}, y_{RP}, z_{RP}) was $a1\,x + b1\,y + c1\,z + d1 = 0$, the equation of J plane covering Landmark LJ (x_{LJ}, y_{LJ}, z_{LJ}), LP (x_{LP}, y_{LP}, z_{LP}) and RP (x_{RP}, y_{RP}, z_{RP}) was $a2\,x + b2\,y + c2\,z + d2 = 0$, and the dihedral angle between H plane and J plane was θ_J.

Where,

$$a1 = (y_{LP}-y_{LO})\,(z_{RP}-z_{LO})-(y_{RP}-y_{LO})\,(z_{LP}-z_{LO}),$$
$$b1 = (z_{LP}-z_{LO})\,(x_{RP}-x_{LO})-(z_{RP}-z_{LO})\,(x_{LP}-x_{LO}),$$
$$c1 = (x_{LP}-x_{LO})\,(y_{RP}-y_{LO})-(x_{RP}-x_{LO})\,(y_{LP}-y_{LO}),$$
$$d1 = -(a1\,x_{LO} + b1\,y_{LO} + c1\,z_{LO}),$$
$$a2 = (y_{LP}-y_{LJ})\,(z_{RP}-z_{LJ})-(y_{RP}-y_{LJ})\,(z_{LP}-z_{LJ}),$$
$$b2 = (z_{LP}-z_{LJ})\,(x_{RP}-x_{LJ})-(z_{RP}-z_{LJ})\,(x_{LP}-x_{LJ}),$$
$$c2 = (x_{LP}-x_{LJ})\,(y_{RP}-y_{LJ})-(x_{RP}-x_{LJ})\,(y_{LP}-y_{LJ}),$$
$$d2 = -(a2\,x_{LJ} + b2\,y_{LJ} + c2\,z_{LJ}).$$

Table 1 Murine anatomical landmarks used in this study

Landmarks	Anatomical positions
LO	Anterior notch on frontal process lateral to infraorbital fissure, left side
LP	Intersection of parietal, temporal and occipital bones, left side
RP	Intersection of parietal, temporal and occipital bones, right side
LJ	Intersection of zygomatic process of maxilla with zygoma, superior surface, left side
LZ	Intersection of zygoma with zygomatic process of temporal, superior aspect, left side
LS	Joining of squamosal body to zygomatic process of squamosal, left side

Thus,

$$\theta_J = \arccos\left(\frac{a1\,a2 + b1\,b2 + c1\,c2}{\sqrt{a1^2 + b1^2 + c1^2}\,\sqrt{a2^2 + b2^2 + c2^2}}\right)$$

Likewise, the degree of the dihedral angles between H plane as well as Z plane (θ_Z) and between H plane as well as S plane (θ_S) was determined.

Thirdly, masseter and temporal muscles were collected from 12 male littermates and weighed according to the procedures reported in an earlier study [29]. The temporal/masseter mass percentage was calculated by dividing the weight of the left temporal muscle by the weight of the left masseter muscle and then multiplying 100.

To identify the expression of Cebpb, mRNA expression of the target gene (Cebpb) was assessed. Tissues used for this purpose were collected from the masseter muscle, the temporal muscle, the zygomatic bone, and the clavicle bone of a $Cebpb^{+/+}$ mouse, respectively. Standard procedures for the preparation of the reverse transcriptase polymerase chain reaction (RT-PCR) were carried out as suggested in the literature [30,31]. Primers applied to perform the RT-PCR technique included murine Cebpb sense (5′-AC ACGTGTAACTGTCAGCCG-3′) and murine Cebpb antisense (5′-GCTCGAAACGGAAAAGGTTC-3′). Specific primers for murine glyceraldehyde-3-phosphate dehydrogenase (Gapdh) were used to check the internal control [32]. The RT-PCR technique was conducted with a GeneAmp PCR System 9700 thermal cycler (Applied Biosystems, Foster City, CA, USA). All procedures were carried out according to the manufacturers' instructions.

Data entry and statistical analysis were conducted with the IBM SPSS Statistics (version 20.0, IBM Corporation, Somers, NY, USA). An independent samples *t*-test method was used to assess the difference in the degree of anatomic dihedral angles between genotypes of Cebpb deficiency and the control ($Cebpb^{+/+}$ mice) [33]. In addition, a paired samples *t*-test method was applied to examine the

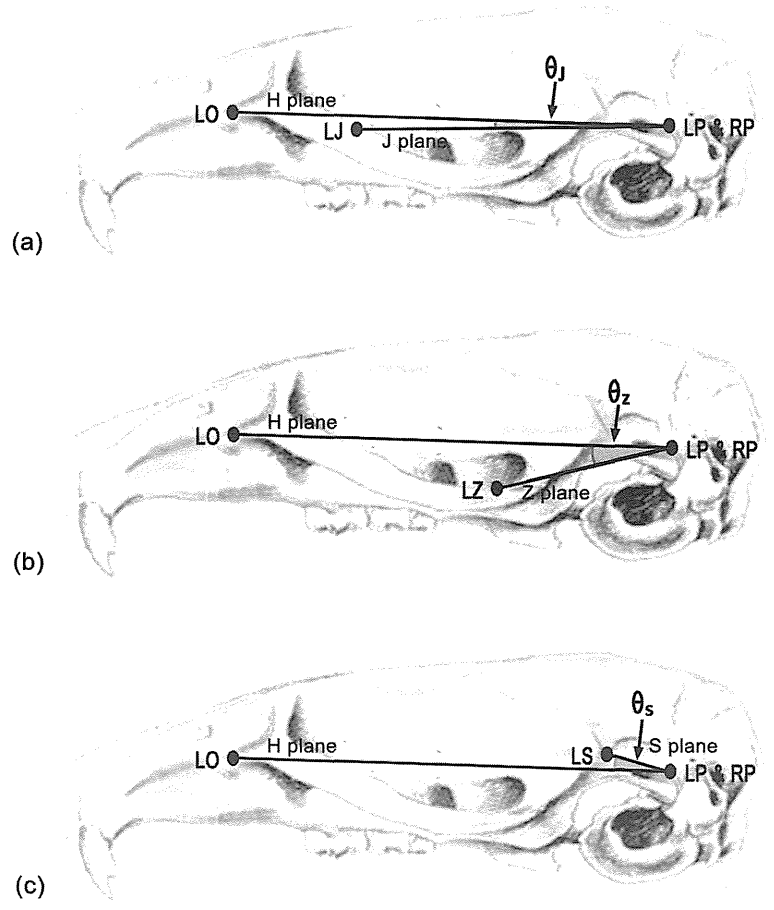

Figure 1 Craniofacial landmarks, established planes and dihedral angles used in this study. (a-c) Landmark LO, LP and RP formed a horizontal reference plane (H plane). **(a)** Landmark LJ, LP and RP formed a jugal plane (J plane). The dihedral angle between J plane and H plane was defined as θ_J. **(b)** Landmark LZ, LP and RP formed a zygomatic plane (Z plane). The dihedral angle between Z plane and H plane was defined as θ_Z. **(c)** Landmark LS, LP and RP formed a squamosal plane (S plane). The dihedral angle between S plane and H plane was defined as θ_S.

difference in the temporal/masseter mass percentage between Cebpb$^{+/-}$ and Cebpb$^{+/+}$ littermates [33]. This paired method has been used to compare dental phenotypes between twins [34]. The level of two-sided significance for all statistical procedures was set at 5%.

Results

Shorter thinner clavicles with a lower radiopacity and a narrower thoracic cage were identified exclusively in Cebpb$^{-/-}$ mice but not Cebpb$^{+/-}$ and/or Cebpb$^{+/+}$ mice (Figure 2). A normal morphology of limb joints was seen in radiographs from animals of all three genotypes. Of further note, mRNA expression of Cebpb was found in the clavicle, the zygoma, the temporal muscle and the masseter muscle (Figure 3).

The mean measurement of θ_Z was 16.3 ± 1.1 degree, 13.0 ± 1.1 degree and 13.4 ± 1.0 degree in Cebpb$^{-/-}$, Cebpb$^{+/-}$ and Cebpb$^{+/+}$ mice, respectively (Table 2). Those animals with a Cebpb$^{-/-}$ genotype showed a larger degree of θ_Z than that were from a Cebpb$^{+/+}$ ($t = 4.964$, $df = 11$, $p < 0.001$) or a Cebpb$^{+/-}$ genetic background ($t = 5.429$, $df = 13$, $p < 0.001$) (Table 2). The latter two genotypes did not differ in the degree of θ_Z ($p = 0.357$) (Table 2). The degree of θ_J in Cebpb$^{-/-}$, Cebpb$^{+/-}$ and Cebpb$^{+/+}$ subjects was separately 6.2 ± 1.1 degree, 5.5 ± 0.7 degree and 6.3 ± 1.7 degree ($p \geq 0.142$) (Table 2). The degree of θ_S in Cebpb$^{-/-}$, Cebpb$^{+/-}$ and Cebpb$^{+/+}$ mice was 3.7 ± 2.2 degree, 3.1 ± 2.2 degree and 5.1 ± 3.3 degree, individually ($p \geq 0.148$) (Table 2). Figure 4 demonstrates a lateral view of dry skulls of a Cebpb$^{-/-}$ and a Cebpb$^{+/+}$ 12-month-old female mice.

The mean weight of the left masseter muscle in Cebpb$^{+/-}$ and Cebpb$^{+/+}$ mice was 113.5 ± 23.9 mg and 120.9 ± 24.4 mg, respectively ($p = 0.362$) (Table 3). The average weight of the left temporal muscle was 36.6 ± 8.8 mg and 32.0 ± 10.1 mg separately in Cebpb$^{+/-}$ and Cebpb$^{+/+}$ subjects ($p = 0.217$) (Table 3). The temporal/masseter mass percentage of Cebpb$^{+/-}$ and Cebpb$^{+/+}$ littermates was 32.3 ± 4.9% and 26.1 ± 6.2%, individually (Table 3). The former displayed a larger percentage than the latter ($t = 3.841$, $df = 5$, $p = 0.012$) (Table 3). Figure 5 shows the difference in the temporal/masseter mass percentage between Cebpb$^{+/-}$ and Cebpb$^{+/+}$ mice by age. The mean of the difference of the temporal/masseter mass percentage between Cebpb$^{+/-}$ and Cebpb$^{+/+}$ amongst young adults (less than 6 months of age), adults (6 to 12 months of age) and mature adults (more than 12 months of age) was 5.66%, 3.29% and 0.55%, respectively.

Discussion

This paper reported phenotypes of mice with Cebpb deficiency, including hypoplastic clavicles, a narrow thoracic cage, a downward tilted zygomatic arch and a comparative mass change of masseter/temporal muscles. In conjunction with our previous findings such as multiple supernumerary teeth and elongated coronoid process in the same species of Cebpb deficient mice [23], these indicated prospective signs of CCD [1-5]. As Cebpb is relevant to expression of Runx2 [18-21] which has been known a determinant of CCD [6], consistency between murine phenotypes of Cebpb deficiency and human manifestations of

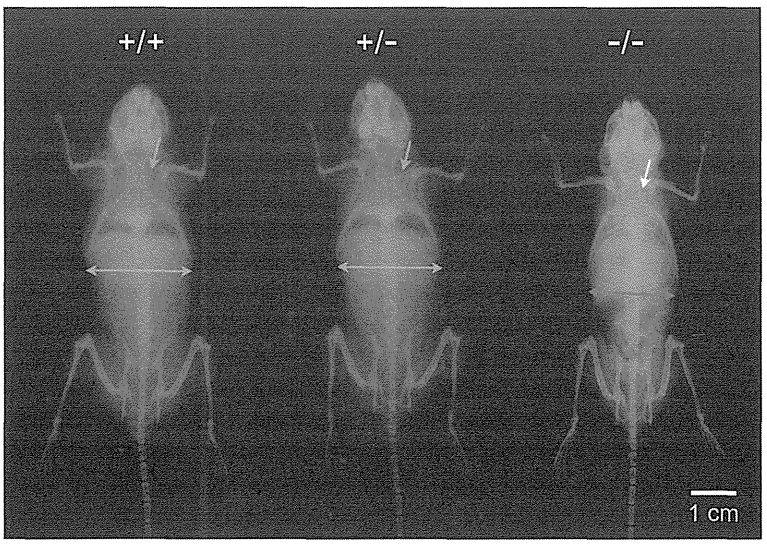

Figure 2 Difference in morphology of clavicles and the thoracic cage. The radiographic image showed a dorsal-ventral view of a Cebpb$^{+/+}$, a Cebpb$^{+/-}$ and a Cebpb$^{-/-}$ 12-month-old mice in this sample. Shorter thinner clavicles with a lower radiopacity (yellow arrow) and a narrow thoracic cage (red arrow) were exclusively seen in Cebpb$^{-/-}$ mice. Due to the limited size of a radiograph film, the radiographic images of the three mice were taken under the same condition separately. The images were displayed without transformation in dimensions, contrast, brightness and/or colour. Scale bar: 1 cm. (n = 23, including 5 Cebpb$^{-/-}$, 10 Cebpb$^{+/-}$ and 8 Cebpb$^{+/+}$ female mice).

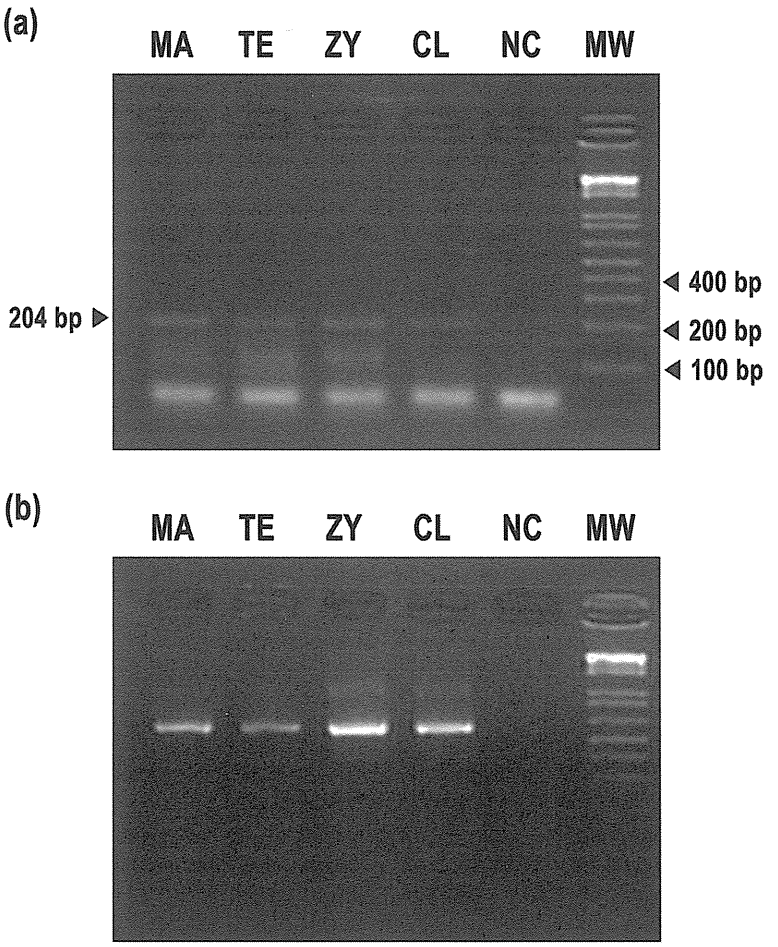

Figure 3 Assessment of mRNA expression in the masseter muscle (MA), the temporal muscle (TE), the zygomatic bone (ZY), the clavicle (CL) and a negative control (NC) with a RT-PCR technique. The size of the molecular weight markers (MW) is displayed on the right, which is given in base pairs (bp). **(a)** Cebpb expression was identified in MA, TE, ZY and CL of a Cebpb$^{+/+}$ adult mouse. **(b)** Gapdh, as an internal control, was detected in the same sites of the mouse.

Table 2 Means of dihedral angles by genotypes in 12-month-old female mice

		Cebpb$^{+/+}$ (n = 8)	Cebpb$^{+/-}$ (n = 10)	Cebpb$^{-/-}$ (n = 5)	All (n = 23)
θ_J		6.3 ± 1.7	5.5 ± 0.7	6.2 ± 1.1	5.9 ± 1.2
p values	$^{+/+}$vs $^{+/-}$	0.227			
	$^{+/-}$ vs $^{-/-}$		0.142		
	$^{-/-}$ vs $^{+/+}$			0.923	
θ_Z		13.4 ± 1.0	13.0 ± 1.1	16.3 ± 1.1	13.9 ± 1.7
p values	$^{+/+}$vs $^{+/-}$	0.357			
	$^{+/-}$ vs $^{-/-}$		<0.001*		
	$^{-/-}$ vs $^{+/+}$			<0.001*	
θ_S		5.1 ± 3.3	3.1 ± 2.2	3.7 ± 2.2	3.9 ± 2.7
p values	$^{+/+}$vs $^{+/-}$	0.148			
	$^{+/-}$ vs $^{-/-}$		0.432		
	$^{-/-}$ vs $^{+/+}$			0.633	

*p < 0.001.

RUNX2 insufficiency implies a potential effect of Cebpb on occurrence of CCD in mice. Of further note, Hirata *et al* demonstrated a similar osteogenic pattern between Cebpb$^{-/-}$Runx2$^{+/+}$ and Cebpb$^{+/+}$Runx2$^{+/-}$ mice [20]. The former was the same Cebpb$^{-/-}$ genotype used in our study and the latter indicated the genotype of CCD [6]. Thus, the resemblance in impaired osteogenesis indicates an association of Cebpb deficiency with CCD. This shows a potential answer to the CCD cases that were free of RUNX2 mutations as mentioned earlier [6].

The current study found hypoplastic clavicles only in Cebpb$^{-/-}$ mice. This agreed with a recent study showing a similar finding [20]. Furthermore, our study identified a narrower thoracic cage in Cebpb$^{-/-}$ mice and this has never been reported in literature. Since Cebpb expression in clavicles was detected in our sample and ossification of clavicles as well as ribs did not complete until a maturer age [35], delayed bone formation due to Cebpb

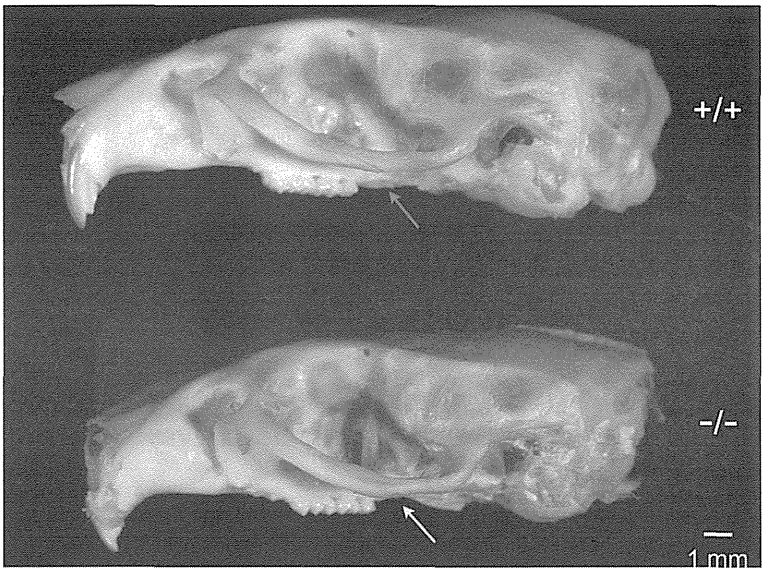

Figure 4 Difference in tilt angulation of the zygomatic arch. The photographic image showed a lateral view of dry skulls respectively collected from a Cebpb$^{+/+}$ and a Cebpb$^{-/-}$ 12-month-old mice. A downward tilt of the zygomatic arch in the Cebpb$^{-/-}$ mouse was confirmed by the morphology of the dry skull (yellow arrow). Scale bar: 1 mm. (n = 23, including 5 Cebpb$^{-/-}$, 10 Cebpb$^{+/-}$ and 8 Cebpb$^{+/+}$ female mice).

deficiency [19] could thereby result in clavicular hypoplasia and a narrowed ribcage.

This study has demonstrated for the first time a downward tilt of the zygomatic arch in Cebpb$^{-/-}$ mice. The larger dihedral angle between Z plane and H plane (θ_Z) identified in Cebpb$^{-/-}$ mice represented that Landmark LZ was located at a more inferior position in the genotype. On the other hand, Landmark LJ and Landmark LS of Cebpb$^{-/-}$ animals were not located at a lower level compared to those of Cebpb$^{+/+}$ and Cebpb$^{+/-}$ mice. This indicated that deformation of the zygomatic arch was limited to the zygoma and not involved with the zygomatic processes of the maxilla and/or the squamosal bone. This finding resembles the feature of a downward tilted zygomatic arch in patients sustaining CCD [3,4]. Although not observed in our mouse model, a past article has suggested an association of human CCD with zygomatic hypoplasia [4]. This may imply a reason why CCD patients displayed a downward inclination of the zygomatic arch. Our detection of Cebpb expression in the zygomatic bone also indicated a potential influence of Cebpb on zygomatic bone formation. Nevertheless, functional interactions among masticatory muscles and craniofacial bones could also contribute to deformity of the zygoma [3,4].

Moreover, this study has reported for the first time a larger temporal/masseter mass percentage in Cebpb$^{+/-}$ mice, which indicated hypotrophy of masseter muscles compared to temporal muscles and/or hypertrophy of temporal muscles compared to masseter muscles. This agreed with a paper which has revealed a volume reduction of masseter muscles in CCD patients [4]. Furuuchi *et al* suggested a causal relationship between hypoplastic zygomatic arch and hypotrophic masseter muscles of CCD cases, based on the anatomic connection [4]. However, this would be difficult to justify the phenotype of masseter muscles in Cebpb$^{+/-}$ mice, since zygomatic deformity was not significant in the genotype. On the other hand, the temporal muscles insert onto the mandibular coronoid process [36] and elongation of the coronoid process in Cebpb$^{+/-}$ mice has been reported by our previous study [23]. Functional activity and muscular development are likely to reciprocally affect growth of the temporal muscle and the coronoid process [3,4]. As

Table 3 Means of weight and mass percentage of masseter and temporal muscles by genotypes in paired male littermates

	Cebpb$^{+/+}$ (n = 6)	Cebpb$^{+/-}$ (n = 6)	All (n = 12)	p value
Weight of the left masseter muscle (mg)	120.9 ± 24.4	113.5 ± 23.9	117.2 ± 23.3	0.362
Weight of the left temporal muscle (mg)	32.0 ± 10.1	36.6 ± 8.8	34.3 ± 9.4	0.217
Temporal/masseter mass percentage (%)	26.1 ± 6.2	32.3 ± 4.9	29.2 ± 6.2	0.012*

*p < 0.05.

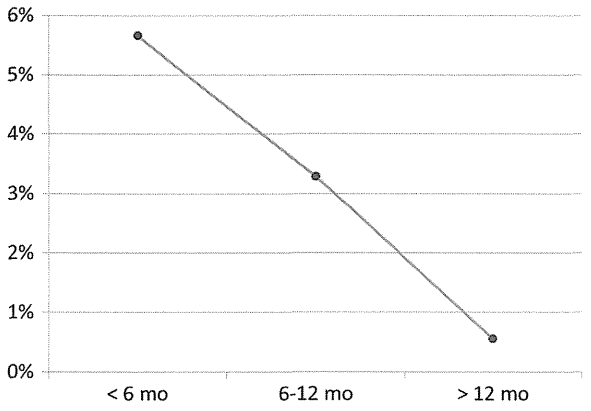

Figure 5 Difference in the temporal/masseter mass percentage between Cebpb$^{+/-}$ and Cebpb$^{+/+}$ mice by age. All Cebpb$^{+/-}$ mice showed a larger temporal/masseter mass percentage than their Cebpb$^{+/+}$ littermates. The mean of the difference of the temporal/masseter mass percentage between Cebpb$^{+/-}$ and Cebpb$^{+/+}$ amongst young adults (less than 6 months of age), adults (6 to 12 months of age) and senior adults (more than 12 months of age) was 5.66%, 3.29% and 0.55%, respectively. (n = 12, including 6 Cebpb$^{+/-}$ and 6 Cebpb$^{+/+}$ male mice).

morphological and physiological adaptations of temporal muscles after masseter myotomy have been reported [37], hypertrophy of the temporal muscle could also result from compensation for the hypotrophic masseter muscles. Figure 5 illustrating a reduced difference in the temporal/masseter mass percentage between Cebpb$^{+/-}$ and Cebpb$^{+/+}$ mice over age might imply that hypotrophy of masseter muscles and/or hypertrophy of temporal muscles in Cebpb$^{+/-}$ subjects occurred at an early age and the difference was compensated and/or corrected following ageing. Cebpb expression detected in masseter and temporal muscles indicated an association of this gene with both muscles. Of further note, unattainability of Cebpb$^{-/-}$ littermates for assessing masticatory muscles was a limit for our research. Although this was due to a high neonatal mortality of Cebpb$^{-/-}$ mice [24], it compromised the inference of a relationship between abnormality of masticatory muscles and the zygomatic arch. Future investigation in the relationships among Cebpb, bone formation the zygomatic arch and development of masticatory muscles is required.

Conclusion

This study has reported prospective signs of CCD, including hypoplastic clavicles, a narrowed thoracic cage, a downward tilt of the zygomatic arch and a comparative mass change between masseter as well as temporal muscles, in mice with Cebpb deficiency. The zygomatic deformation was limited to the zygoma and not involved with the zygomatic processes of the maxilla and/or the squamosal bone. In addition, the difference in the temporal/masseter mass percentage between Cebpb deficiency and wild-type mice decreased over age.

Cebpb has been demonstrated as a key regulator for Runx2 which was related to occurrence of most but not all CCD cases. The data presented here, taken together with the authors' previous study, implicates Cebpb deficiency in some CCD-like phenotypes and this contributes to understanding of the genes involved in the disorder. Succeeding investigation into interactions among Cebpb, Runx2 and musculoskeletal development is indicated.

Competing interests

The authors declare that they have no competing interests.

Authors' contributions

Designing research/study: BH, KT, KB. Performing research/study: BH, PP, HK, YT, KS. Contributing important materials/reagents: KT, MS, SA, AS, KB. Data collection: BH, PP, HK, YT. Data analysis: BH, EJ, PP. Writing paper: BH, EJ. All authors read and approved the final manuscript.

Acknowledgement

The publication was supported with a Japanese Society for the Promotion of Science (JSPS) Postdoctoral Fellowship (P09741) awarded by the JSPS and the Australian Academy of Science. The authors would like to show appreciation to those staff and students who helped in this project. In addition, the paper is indebted to Professor Jen-Shiang Kenny Yu, Dr Yunlong Kang, Dr Kazumasa Nakao, Dr Noriaki Koyama, Dr Hiroko Tsukamoto and Dr Tomoko Goto for helpful discussions. Special thanks to Dr Mei-lan Chen for her assistance in preparation of electronic artwork.

Author details

[1]School of Medicine and Dentistry, James Cook University, Cairns, Australia. [2]Department of Oral and Maxillofacial Surgery, Graduate School of Medicine, Kyoto University, Shogoin-Kawahara-cho 54, Sakyo-ku, Kyoto 606-8507, Japan. [3]Setthasiri Animal Hospital, Bangkok, Thailand. [4]Translational Research Center, Kyoto University Hospital, Kyoto University, Kyoto, Japan. [5]Laboratory of Host Defense, World Premier International Immunology, Frontier Research Center, Osaka University, Osaka, Japan.

Received: 7 April 2014 Accepted: 8 May 2014
Published: 13 May 2014

References

1. Suda N, Hattori M, Kosaki K, Banshodani A, Kozai K, Tanimoto K, Moriyama K: **Correlation between genotype and supernumerary tooth formation in cleidocranial dysplasia.** *Orthod Craniofac Res* 2010, **13**:197–202.
2. Chen BH, Chen LY, Jaw TH, Chao MC: **Cleidocranial dysplasia: a rare case associated with congenital hypothyroidism and severe neonatal hyperbilirubinemia.** *Kaohsiung J Med Sci* 1998, **14**:53–57.
3. McNamara CM, O'Riordan BC, Blake M, Sandy JR: **Cleidocranial dysplasia: radiological appearances on dental panoramic radiography.** *Dentomaxillofac Radiol* 1999, **28**:89–97.
4. Furuuchi T, Kochi S, Sasano T, Iikubo M, Komai S, Igari K: **Morphologic characteristics of masseter muscle in cleidocranial dysplasia: a report of 3 cases.** *Oral Surg Oral Med Oral Pathol Oral Radiol Endod* 2005, **99**:185–190.
5. Rizvi S, Raihan H, Rizvi T: **Cleidocranial dysplasia - a case report.** *Biomed Res* 2006, **17**:129–132.
6. Mundlos S, Otto F, Mundlos C, Mulliken JB, Aylsworth AS, Albright S, Lindhout D, Cole WG, Henn W, Knoll JH, Owen MJ, Mertelsmann R, Zabel BU, Olsen BR: **Mutations involving the transcription factor CBFA1 cause cleidocranial dysplasia.** *Cell* 1997, **89**:773–779.
7. Liu JC, Lengner CJ, Gaur T, Lou Y, Hussain S, Jones MD, Borodic B, Colby JL, Steinman HA, van Wijnen AJ, Stein JL, Jones SN, Stein GS, Lian JB: **Runx2 protein expression utilizes the Runx2 P1 promoter to establish osteoprogenitor cell number for normal bone formation.** *J Biol Chem* 2011, **286**:30057–30070.

8. Ducy P, Zhang R, Geoffroy V, Ridall AL, Karsenty G: **Osf2/Cbfa1: a transcriptional activator of osteoblast differentiation.** *Cell* 1997, **89**:747–754.
9. Gibert Y, Bernard L, Debiais-Thibaud M, Bourrat F, Joly J-S, Pottin K, Meyer A, Retaux S, Stock DW, Jackman WR, Seritrakul P, Begemann G, Laudet V: **Formation of oral and pharyngeal dentition in teleosts depends on differential recruitment of retinoic acid signaling.** *FASEB J* 2010, **24**:3298–3309.
10. Åberg T, Wang X-P, Kim J-H, Yamashiro T, Bei M, Rice R, Ryoo HM, Thesleff I: **Runx2 mediates FGF signaling from epithelium to mesenchyme during tooth morphogenesis.** *Dev Biol* 2004, **270**:76–93.
11. Hatch NE, Li Y, Franceschi RT: **FGF2 Stimulation of the pyrophosphate-generating enzyme, PC-1, in pre-osteoblast cells is mediated by RUNX2.** *J Bone Miner Res* 2009, **24**:652–662.
12. Diehl AM: **Roles of CCAAT/enhancer-binding proteins in regulation of liver regenerative growth.** *J Biol Chem* 1998, **273**:30843–30846.
13. Seagroves TN, Krnacik S, Raught B, Gay J, Burgess-Beusse B, Darlington GJ, Rosen JM: **C/EBPβ, but not C/EBPα, is essential for ductal morphogenesis, lobuloalveolar proliferation, and functional differentiation in the mouse mammary gland.** *Genes Dev* 1998, **12**:1917–1928.
14. Poli V: **The role of C/EBP isoforms in the control of inflammatory and native immunity functions.** *J Biol Chem* 1998, **273**:29279–29282.
15. Tanaka T, Akira S, Yoshida K, Umemoto M, Yoneda Y, Shirafuji N, Fujiwara H, Suematsu S, Yoshida N, Kishimoto T: **Targeted disruption of the NF-IL6 gene discloses its essential role in bacteria killing and tumor cytotoxicity by macrophages.** *Cell* 1995, **80**:353–361.
16. Kagan BL, Henke RT, Cabal-Manzano R, Stoica GE, Nguyen Q, Wellstein A, Riegel AT: **Complex regulation of the fibroblast growth factor-binding protein in MDA-MB-468 breast cancer cells by CCAAT/enhancer-binding protein β.** *Cancer Res* 2003, **63**:1696–1705.
17. Tang Q-Q, Otto TC, Lane MD: **CCAAT/enhancer-binding protein β is required for mitotic clonal expansion during adipogenesis.** *Proc Natl Acad Sci U S A* 2003, **100**:850–855.
18. Wiper-Bergeron N, St-Louis C, Lee JM: **CCAAT/enhancer binding protein β abrogates retinoic acid-induced osteoblast differentiation via repression of Runx2 Transcription.** *Mol Endocrinol* 2007, **21**:2124–2135.
19. Tominaga H, Maeda S, Hayashi M, Takeda S, Akira S, Komiya S, Nakamura T, Akiyama H, Imamura T: **CCAAT/enhancer-binding protein β promotes osteoblast differentiation by enhancing Runx2 activity with ATF4.** *Mol Biol Cell* 2008, **19**:5373–5386.
20. Hirata M, Kugimiya F, Fukai A, Saito T, Yano F, Ikeda T, Mabuchi A, Sapkota BR, Akune T, Nishida N, Yoshimura N, Nakagawa T, Tokunaga K, Nakamura K, Chung UI, Kawaguchi H: **C/EBPβ and RUNX2 cooperate to degrade cartilage with MMP-13 as the target and HIF-2α as the inducer in chondrocytes.** *Hum Mol Genet* 2012, **21**:1111–1123.
21. Gutierrez S, Javed A, Tennant DK, van Rees M, Montecino M, Stein GS, Stein JL, Lian JB: **CCAAT/enhancer-binding proteins (C/EBP) β and δ activate osteocalcin gene transcription and synergize with Runx2 at the C/EBP element to regulate bone-specific expression.** *J Biol Chem* 2002, **277**:1316–1323.
22. Savage T, Bennett T, Huang YF, Kelly PL, Durant NE, Adams DJ, Mina M, Harrison JR: **Mandibular phenotype of p20C/EBPβ transgenic mice: reduced alveolar bone mass and site-specific dentin dysplasia.** *Bone* 2006, **39**:552–564.
23. Huang B, Takahashi K, Sakata-Goto T, Kiso H, Togo Y, Saito K, Tsukamoto H, Sugai M, Akira S, Shimizu A, Bessho K: **Phenotypes of CCAAT/enhancer-binding protein beta deficiency: hyperdontia and elongated coronoid process.** *Oral Dis* 2013, **19**:144–150.
24. Bai T, Tanaka T, Yukawa K, Umesaki N, Matsumoto M, Akira S: **Impaired postnatal development in C/EBP beta deficient mice.** *J Reprod Dev* 2006, **52**:645–649.
25. Richtsmeier JT, Baxter LL, Reeves RH: **Parallels of craniofacial maldevelopment in down syndrome and Ts65Dn mice.** *Dev Dyn* 2000, **217**:137–145.
26. Uchida Y, Goto M, Katsuki T, Akiyoshi T: **Measurement of the maxilla and zygoma as an aid in installing zygomatic implants.** *J Oral Maxillofac Surg* 2001, **59**:1193–1198.
27. Cook M: *The Anatomy of the Laboratory Mouse.* 1st edition. New York: Academic; 1965.
28. Sidebotham TH: *The A to Z of Mathematics: A Basic Guide.* Hoboken, NJ: Wiley; 2003.
29. Tsai CY, Yang LY, Chen KT, Chiu WC: **The influence of masticatory hypofunction on developing rat craniofacial structure.** *Int J Oral Maxillofac Surg* 2010, **39**:593–598.
30. Salingcarnboriboon R, Tsuji K, Komori T, Nakashima K, Ezura Y, Noda M: **Runx2 is a target of mechanical unloading to alter osteoblastic activity and bone formation in vivo.** *Endocrinology* 2006, **147**:2296–2305.
31. Kawagishi H, Wakoh T, Uno H, Maruyama M, Moriya A, Morikawa S, Okano H, Sherr CJ, Takagi M, Sugimoto M: **Hzf regulates adipogenesis through translational control of C/EBP alpha.** *EMBO J* 2008, **27**:1481–1490.
32. Suzuki T, Higgins PJ, Crawford DR: **Control selection for RNA quantitation.** *Biotechniques* 2000, **29**:332–337.
33. Altman D: *Practical Statistics for Medical Research.* London: Chapman and Hall; 1991.
34. Mihailidis S, Woodroffe SN, Hughes TE, Bockmann MR, Townsend GC: **Patterns of asymmetry in primary tooth emergence of Australian twins.** *Front Oral Biol* 2009, **13**:110–115.
35. Garamendi PM, Landa MI, Botella MC, Alemán I: **Forensic age estimation on digital x-ray images: medial epiphyses of the clavicle and first rib ossification in relation to chronological age.** *J Forensic Sci* 2011, **56**:S3–S12.
36. Dubrul E: *Sicher and Dubrul's Oral Anatomy.* 8th edition. Ishiyaku Euroamerica: St. Louis; 1988.
37. Maxwell L, Carlson D, McNamara JJ, Faulkner J: **Adaptation of the masseter and temporalis muscles following alteration in length, with or without surgical detachment.** *Anat Rec* 1981, **200**:127–137.

doi:10.1186/1423-0127-21-44
Cite this article as: Huang *et al.*: Prospective signs of cleidocranial dysplasia in Cebpb deficiency. *Journal of Biomedical Science* 2014 **21**:44.

PLOS | ONE

Interactions between BMP-7 and USAG-1 (Uterine Sensitization-Associated Gene-1) Regulate Supernumerary Organ Formations

Honoka Kiso[1], Katsu Takahashi[1]*, Kazuyuki Saito[1], Yumiko Togo[1], Hiroko Tsukamoto[1], Boyen Huang[2], Manabu Sugai[3], Akira Shimizu[4], Yasuhiko Tabata[5], Aris N. Economides[6], Harold C. Slavkin[7], Kazuhisa Bessho[1]

1 Department of Oral and Maxillofacial Surgery, Graduate School of Medicine, Kyoto University, Shogoin-Kawahara-cho, Sakyo-ku, Kyoto, Japan, **2** Department of Paediatric Dentistry, School of Medicine and Dentistry, James Cook University, Cairns, Australia, **3** Translational Research Center, Kyoto University Hospital, Shogoin-Kawahara-cho, Sakyo-ku, Kyoto, Japan, **4** Laboratory of Host Defense, World Premier International Immunology Frontier Research Center, Osaka University, Suita, Osaka, Japan, **5** Department of Biomaterials, Institute for Frontier Medical Sciences, Kyoto University, Kyoto, Japan, **6** Regeneron Pharmaceuticals, Tarrytown, New York, United States of America, **7** Center for Craniofacial Molecular Biology, Division of Biomedical Sciences, Ostrow School of Dentistry, University of Southern California, Los Angeles, California, United States of America

Abstract

Bone morphogenetic proteins (BMPs) are highly conserved signaling molecules that are part of the transforming growth factor (TGF)-beta superfamily, and function in the patterning and morphogenesis of many organs including development of the dentition. The functions of the BMPs are controlled by certain classes of molecules that are recognized as BMP antagonists that inhibit BMP binding to their cognate receptors. In this study we tested the hypothesis that USAG-1 (uterine sensitization-associated gene-1) suppresses deciduous incisors by inhibition of BMP-7 function. We learned that USAG-1 and BMP-7 were expressed within odontogenic epithelium as well as mesenchyme during the late bud and early cap stages of tooth development. USAG-1 is a BMP antagonist, and also modulates Wnt signaling. USAG-1 abrogation rescued apoptotic elimination of odontogenic mesenchymal cells. BMP signaling in the rudimentary maxillary incisor, assessed by expressions of Msx1 and Dlx2 and the phosphorylation of Smad protein, was significantly enhanced. Using explant culture and subsequent subrenal capsule transplantation of E15 USAG-1 mutant maxillary incisor tooth primordia supplemented with BMP-7 demonstrated in USAG-$1^{+/-}$ as well as USAG-$1^{-/-}$ rescue and supernumerary tooth development. Based upon these results, we conclude that USAG-1 functions as an antagonist of BMP-7 in this model system. These results further suggest that the phenotypes of USAG-1 and BMP-7 mutant mice reported provide opportunities for regenerative medicine and dentistry.

Citation: Kiso H, Takahashi K, Saito K, Togo Y, Tsukamoto H, et al. (2014) Interactions between BMP-7 and USAG-1 (Uterine Sensitization-Associated Gene-1) Regulate Supernumerary Organ Formations. PLoS ONE 9(5): e96938. doi:10.1371/journal.pone.0096938

Editor: Michael Klymkowsky, University of Colorado, Boulder, United States of America

Received December 18, 2013; **Accepted** April 13, 2014; **Published** May 9, 2014

Funding: This work was supported by Grant-in-Aid for Scientific Research(C): 22592213 and 25463081 and A-STEP (Adaptable & Seamless Technology Transfer Program through Target-driven R&D) FS stage: AS231Z01061G and AS242Z02645Q. The funders had no role in study design, data collection and analysis, decision to publish, or preparation of the manuscript.

Competing Interests: Aris N. Economides is employed by Regeneron Pharmaceuticals, Inc. There are no patents, products in development or marketed products to declare. This does not alter the authors' adherence to all the PLOS ONE policies on sharing data and materials, as detailed online in the guide for authors.

* E-mail: takahask@kuhp.kyoto-u.ac.jp

Introduction

A significant number of discoveries have also been advanced for the establishment of tooth position and patterning, critical developmental pathways that regulate cell and tissue formations, extracellular matrix formations, biomineralization, and the associated genes and gene families (see recent reviews by [1–3]).

A curious clinical aberration during craniofacial morphogenesis is the patterning and subsequent organogenesis of supernumerary tooth organs. The term "supernumerary teeth" describes the production of more than the normal number of teeth in the human primary or permanent dentition. The prevalence of supernumerary teeth on a population basis ranges from 0.1 to 3.6% [4], [5]. In contrast, normal mouse development presents a monophyodont dentition composed of one incisor and three molars in each quadrant. Unlike humans, mice have only molar and incisor tooth organs separated by a "toothless region" termed the diastema. In addition, mice have a single primary dentition and their teeth are not replaced.

The animal models have significantly contributed towards understanding the molecular and developmental biology of human craniofacial biology (see treatise by [6]). A number of mouse mutants provide insights into the supernumerary tooth formation [7–20]. Several mechanisms by which supernumerary tooth might arise in mice have been proposed [21–26]. One plausible explanation for supernumerary tooth formation is the rescue of tooth rudiments such as within the diastema region [26–29] or maxillary deciduous incisor [15,30]. During early stages of mouse tooth development transient vestigial tooth buds develop in the diastema area; developing to the bud stage yet later regressing and

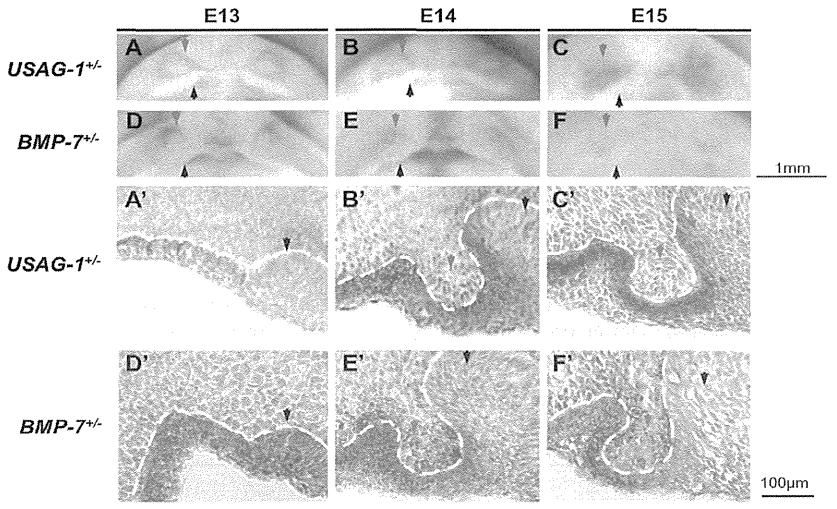

Figure 1. BMP-7 co-localization with USAG-1 in the mesenchymal and epithelial cells of maxillary rudimentary incisor. (A–F) Whole-mount X-Gal expression in tooth germs of E13 –15 maxillary. (A'–F') Parasagittal sections (anterior to the left) of the tooth germs from panels A–F show X-Gal expression in the rudimentary incisor epithelium. USAG-1 (A–C, A'–C') and BMP-7 (D–F, D'–F') were expressed in the tooth organ of rudimentary maxillary incisor (red arrow) in addition to the tooth organ of characteristic incisor (black arrow). At E13, USAG-1 and BMP-7 transcripts were prominent in the labial epithelium in addition to the dental epithelium (A, D, A' and D'). At E14, USAG-1 and BMP-7 started to be expressed in the mesenchymal cells of the maxillary rudimentary incisor to the surface of the epithelium (B, E, B' and E'). At E15, the expression of both USAG-1 and BMP-7 increased in the mesenchymal cells of the maxillary rudimentary incisor (C, F, C' and F'). BMP-7 co-localized with USAG-1 in the area of the tooth germ of maxillary rudimentary incisor in addition to the tooth organ of regular maxillary incisor. White dotted line indicates the interface between epithelium and mesenchyme.
doi:10.1371/journal.pone.0096938.g001

disappear by apoptosis, or merge with the mesial crown of the adjacent first molar tooth organ [26,28,29]. The rudimentary maxillary incisor regressed by apoptotic elimination of mesenchymal cells [15]. Recently, we demonstrate that USAG-1(also known as Sostdc1, ectodin, and Wise) -deficient mouse model has supernumerary incisors in the maxillary and mandible, a fused tooth in the maxillary and mandibular molar regions, and a supernumerary tooth was also located in front of the first mandibular molar [15]. Increased BMP signaling results in supernumerary teeth in the USAG-1-deficient mouse model [21].

USAG-1 is a bone morphogenetic protein antagonist that is expressed at high levels in the kidney and inhibits BMP-7 bioactivity [31,32]. Bone morphogenetic protein-7 is a 35-kDa homodimeric protein, and plays an important role in the specification and patterning of the early embryo and functions to regulate apoptosis in many developmental processes [33,34]. BMP-4 as well as BMP-2 and BMP-7 are expressed in the limb bud [35], and in cranial neural crest cells [36,37] with associated induction of apoptosis. Curiously, BMP-4 and BMP-7 prevent apoptosis of the metanephric mesenchyme during kidney development [38,39]. Further, as the result from renal injury, BMP-7 inhibits apoptosis of proximal tubule epithelial cells [40]. It has been reported that USAG-1 binds to BMP-7 and inhibits the apoptosis-protective actions of BMP-7 in the kidney [41]. BMP-7 null mice present a craniofacial syndrome including severe eye defects, including anophthalmia and microphthalmia, skeletal and renal anomalies, and die shortly after birth [38,42–44]. Meanwhile, absence or agenesis of the maxillary teeth in conditional BMP-7 null mice has recently been reported [44].

The purpose of these present investigations is to test the hypothesis that USAG-1 suppresses deciduous incisors by inhibition of BMP-7 function. If valid, our results would also demonstrate that a novel BMP-7 antagonist functioning as a negative regulator in BMP functions can assist towards advancing regenerative medicine and dentistry.

Materials and Methods

Ethic Statement

All procedures were approved by the Animal Care Committee at Kyoto University.

Mouse strains

USAG-1/LacZ mice [45] and BMP-7/LacZ mice [46] were used in this study. USAG-1/LacZ mice were on a C57Bl6/J background and BMP-7/LacZ mice were on an Imprinting Control Region (ICR) background. USAG-$1^{-/-}$/BMP-$7^{-/-}$ mice were generated by crossing two lines of mice. To eliminate the influence of mouse background, only F2 progeny was analysed. Embryos were obtained by timed mating, day E0 started from midnight prior to finding a vaginal plug.

Whole-mount LacZ staining

Embryos thus obtained were briefly washed in Hank's solution and immediately fixed in cold fixative solution [2% formaldehyde, 0.2% glutaraldehyde, 0.01% sodium deoxycholate and 0.02% NP-4 in phosphate buffer saline (PBS)] for 2 min. They were subsequently washed several times with PBS/2 mM $MgCl_2$, and stained for several hours to overnight in x-gal staining solution (0.1 M phosphate buffer pH 7.3, 2 mM $MgCl_2$, 0.01% sodium deoxycholate, 0.02% NP-40, 5 mM $K_3Fe(CN)_6$, 5 mM $K_4Fe(CN)_6$ and 1 mg/ml x-gal) at room temperature in the dark.

Embryos were then washed in PBS, post-fixed in 1% paraformaldehyde (PFA) and dissected for macroscopic analysis.

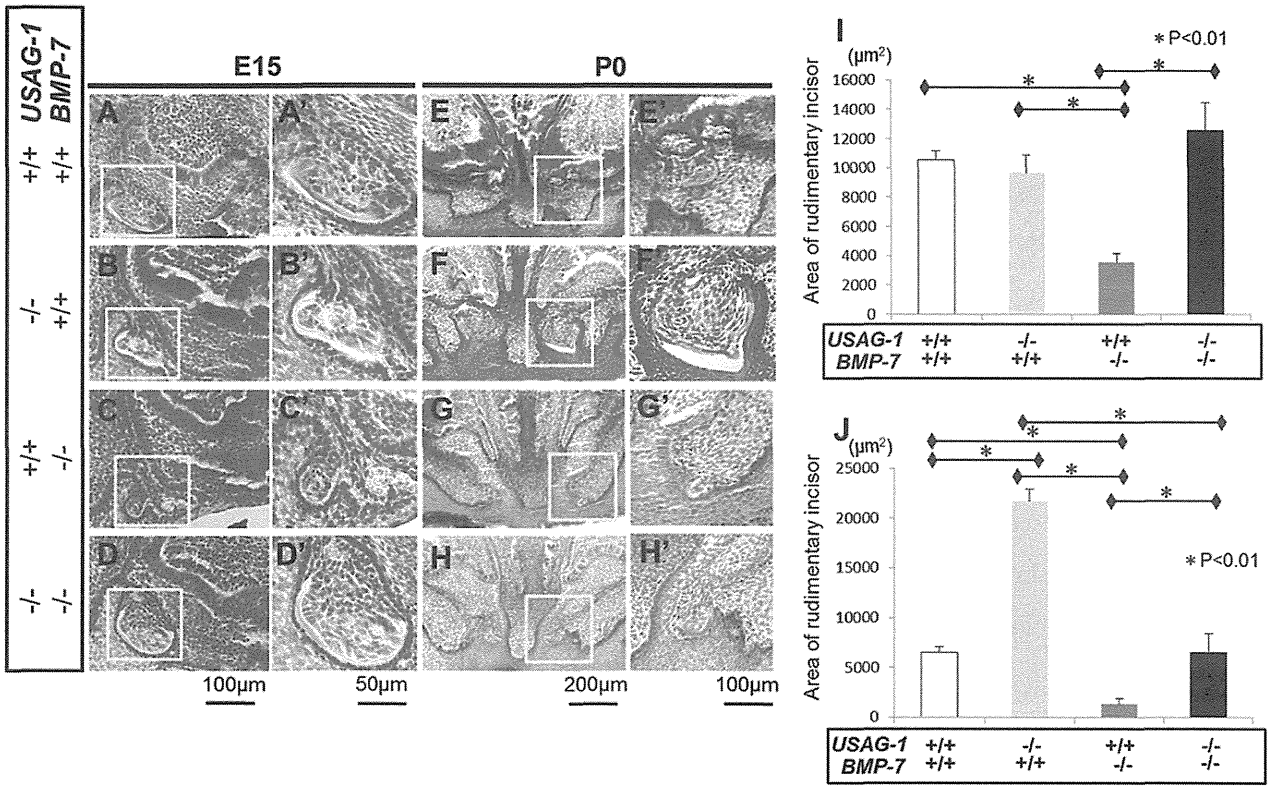

Figure 2. USAG-1 antagonises BMP-7 in maxillary supernumerary incisors formation. Sagittal sections of E15 (A–D) embryos and frontal sections of mice on the day of birth (E–H). (A'–H') Higher magnification of the boxed regions in (A–H). USAG-$1^{+/+}$/BMP-$7^{+/+}$, (A, A', E, E'); USAG-$1^{-/-}$/BMP-$7^{+/+}$, (B, B', F, F'); USAG-$1^{+/+}$/BMP-$7^{-/-}$, (C, C', G, G') and USAG-$1^{-/-}$/BMP-$7^{-/-}$ (D, D', H, H'). The area of rudimentary incisor was measured in transverse sections of USAG-$1^{+/+}$/BMP-$7^{+/+}$ (white bars), USAG-$1^{-/-}$/BMP-$7^{+/+}$ (right grey bars), USAG-$1^{+/+}$/BMP-$7^{-/-}$ (dark grey bars) and USAG-$1^{-/-}$/BMP-$7^{-/-}$ (black bars) mice (n = 5) in E15 (I) and P0 (J). At E15, the area of the maxillary deciduous incisor was identified in wild type as well as all mutant mice in the labial border of the epithelial invagination. The size of rudimentary incisor is similar except USAG-$1^{+/+}$/BMP-$7^{-/-}$ at E15 (A, A', B, B', C, C', D, D' and I).Rudimentary tooth primordia in USAG-$1^{-/-}$/BMP-$7^{-/-}$ and USAG-$1^{+/+}$/BMP-$7^{+/+}$ regressed and its size became smaller at birth, whereas the teeth in USAG-$1^{-/-}$/BMP-$7^{+/+}$ continued to develop and enamel organ was formed (E, E', F, F', H, H' and J).
doi:10.1371/journal.pone.0096938.g002

LacZ staining on sections

Embryos obtained from timed mating were fixed in 4% PFA, equilibrated in 25% sucrose and embedded in water soluble glycols and resins (Miles Laboratories, Elkhart, IN). Sections of 8 μm were cut and stained for LacZ following the same protocol as for whole-mount staining except that they were fixed for 5 min and stained at 37°C. Sections were post-fixed in 1% PFA, counter-stained with nuclear fast red, mounted with glycerine, covered and sealed with nail polish.

Analysis of tooth phenotype

Embryos and neonates were fixed in 4% PFA and embedded in paraffin. Sections of 7 mm were cut and stained with haematoxylin and eosin. The area of the maxillary rudimentary incisor tooth of all mice was measured using Image J software (US NIH, Bethesda, MD, USA).

Detection of apoptosis

Apoptosis was detected by the terminal deoxynucleotidyl transferase-mediated dUTP nick end-labelling method using an ApopTag Plus In Situ Apoptosis Detection Kit-Fluorescein (Oncor, Rockville, MD) according to the manufacturer's specifications. Specimens were briefly washed, dehydrated through a graded series of ethanol in PBS and subjected to labelling with an ApopTag Plus In Situ Apoptosis Detection Kit. Cell nuclei were counter stained with instant-blue nuclear probe fluorescing (455 nm) compound (SouthernBiotech, Birmingham, AL).

Immunohistochemistry

Paraffin-embedded sections of embryos were immunostained with primary rabbit polyclonal antibodies against phosphorylated Smad 1/5/8 (1:100; Cell Signaling Technology, Beverly, MA); goat polyclonal antibodies against phosphorylated Smad 2/3 (1:100; Santa Cruz Biotechnology Inc., Santa Cruz, CA); and secondary biotinylated anti-rabbit, goat and mouse antibodies (Nichirei Bioscience, Tokyo, Japan), as previously described [41,47,48]. Sections were then counter-stained with haematoxylin, dehydrated in a graded series of ethanol and xylene, and covered with coverslips.

Whole mount *in situ* hybridization

Specific probes for mouse Dlx2 and Msx1 were obtained by the reverse transcription-polymerase chain reaction method and confirmed by direct sequencing. Digoxigenin (DIG)-labelled sense and antisense riboprobes were prepared by the in vitro transcription of phagemids using an RNA Transcription Kit (Stratagene, La Jolla, CA) according to the manufacturer's specifications. Whole mount in situ hybridization was performed according to the

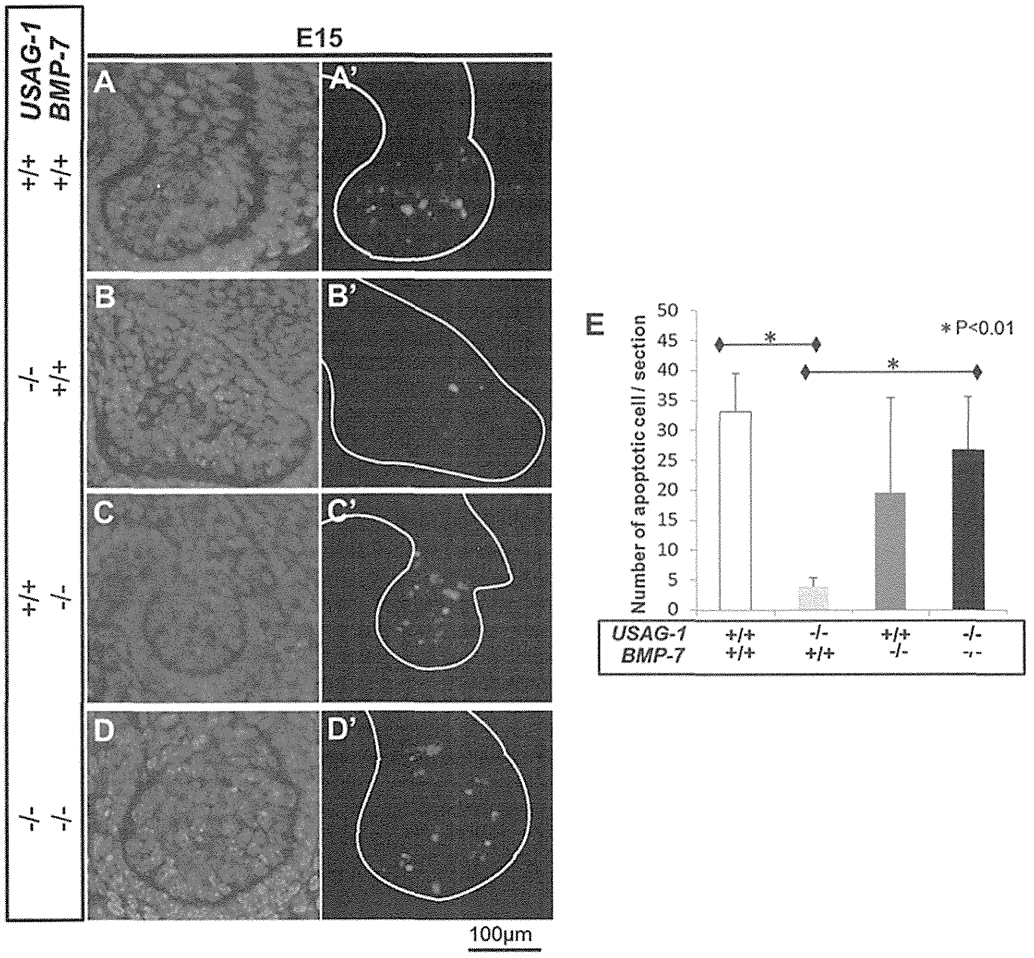

Figure 3. USAG-1 abrogation rescues apoptotic elimination of odontogenic mesenchymal cells. Sagittal sections of E15 embryo maxillary rudimentary incisor in transferase-mediated dUTP nick end-labelling method (TUNEL) staining; Cell nuclei were counterstained with Dapi (A–D), and TUNEL-positive cells in mesenchymal cells of maxillary rudimentary incisor (A'–D'). USAG-$1^{+/+}$/BMP-$7^{+/+}$, (A, A'); USAG-$1^{-/-}$/BMP-$7^{+/+}$, (B, B'); USAG-$1^{+/+}$/BMP-$7^{-/-}$, (C, C') and USAG-$1^{-/-}$/BMP-$7^{-/-}$ (D, D'). White line indicates the interface between epithelium and mesenchyme. The number of TUNEL-positive cells per section was counted in transverse section of USAG-$1^{+/+}$/BMP-$7^{+/+}$ (white bars), USAG-$1^{-/-}$/BMP-$7^{+/+}$ (right grey bars), USAG-$1^{+/+}$/BMP-$7^{-/-}$ (dark grey bars), and USAG-$1^{-/-}$/BMP-$7^{-/-}$ (black bars) mice (n = 3; E). USAG-1 abrogation rescued the apoptotic elimination of odontogenic mesenchymal cells in the tooth primordia of rudimentary maxillary incisor at E15, whereas these size are comparable (A, A', B and B'). The apoptotic odontogenic mesenchymal cells in USAG-$1^{-/-}$/BMP-$7^{-/-}$ are similar to USAG-$1^{+/+}$/BMP-$7^{+/+}$ in contrast to those in USAG-$1^{-/-}$/BMP-$7^{+/+}$ (A, A', B, B', D and D').
doi:10.1371/journal.pone.0096938.g003

following protocol. Briefly, specimens were fixed in 4% PFA in PBS and permeabilized with Radioimmunoprecipitation assay buffer, following which they were hybridized overnight with 1 mg/ml DIG-labelled riboprobes at 70 °C. The specimens were then washed, blocked, and further incubated with alkaline phosphatase-conjugated anti-DIG (Boehringer Mannheim, Indianapolis, IN) at a 1:2000 dilution at 4°C overnight. The bound alkaline phosphatase was visualized after incubation with nitro blue tetrazolium (NBT)/5-bromo-4-chloro-3-indolyl phosphate (BCIP) substrate.

Organ culture and subrenal capsule assay

E15 USAG-1-deficient, heterozygous, and wild-type mice incisors were dissected in Hank's solution under a stereomicroscope. Tooth explants were cultured for one day on Nucleopore filters at 37°C in 5% CO_2 in a Trowell-type organ culture containing BGJb with 10% fetal bovine serum. The explants were then transplanted beneath the kidney capsule. Gelatin hydrogel microspheres (MedGel, Osaka, Japan) with <30 μm diameter were prepared as described previously [49,50]. The microspheres were incubated with PBS (control) or PBS containing BMP-7 (R&D Systems, Minneapolis, MN; 200 ng/ml) for 1 h at room temperature. Subcutaneous implantation was performed using a pair of fine tweezers under the stereomicroscope. Animals were sacrificed at 19 days after transplantation. Explants were fixed in 10% PFA and processed for immunohistochemistry.

Statistical analysis

Data were analysed by two-way analysis of variance and Student's t-test, and significance was determined at a confidence level of $p<0.01$. All experiments were performed in triplicate.

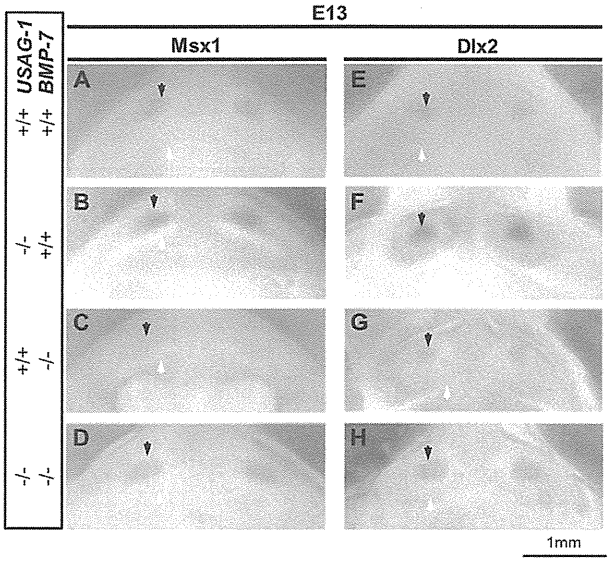

Figure 4. Intensive expression of Msx1 and Dlx2 in the rudimentary incisors of USAG-1 and BMP-7 mutants. Occlusal view of the tooth organ of rudimentary maxillary incisor primordium at E13 on whole mount in situ hybridization (A–H). Msx1 (A–D) and Dlx2 (E–H) transcription factors were expressed in the tooth organ of rudimentary maxillary incisor (black arrow) in addition to the tooth organ of characteristic incisor (white arrow). At E13, Msx1 and Dlx2 expression in the rudimentary maxillary incisors of USAG-$1^{-/-}$/BMP-$7^{-/-}$ mice was comparable with that of USAG-$1^{+/+}$/BMP-$7^{+/+}$, whereas that of USAG-$1^{-/-}$/BMP-$7^{+/+}$ appeared more intense as compared with that of controls (A–H).
doi:10.1371/journal.pone.0096938.g004

Results

BMP-7 co-localization with USAG-1 in mesenchymal and epithelial cells of the maxillary rudimentary incisor tooth germ

USAG-1 transcript expression was detected in the area of the maxillary rudiment incisor tooth germ in addition to the regular maxillary incisor tooth organ by in situ hybridization [15]. We examined the expression of USAG-1 and BMP-7 in the maxillary rudiment incisor tooth germ at E13–15 using USAG-$1^{+/LacZ}$ and BMP-$7^{+/LacZ}$ mice. At E13 (late bud stage), USAG-1 and BMP-7 transcripts were prominent in the labial epithelium in addition to the enamel organ epithelium (Fig. 1A, D, A' and D). At E14 (early cap stage), USAG-1 and BMP-7 transcripts were first detected in the mesenchymal cells of the maxillary rudimentary incisor (Fig. 1B, E, B' and E'). At E15 (cap stage), USAG-1 and BMP-7 expression increased in the mesenchymal cells of the maxillary incisor tooth organ (Fig. 1C, F, C' and F'). BMP-7 co-localized with USAG-1 in the area of the maxillary rudiment incisor tooth organ in addition to the conventional maxillary incisor tooth organ.

USAG-1 functions as a BMP-7 antagonist in maxillary supernumerary incisor formation

BMP-7 deficient mice die shortly after birth due to severe renal hypoplasia [38,42]. To test the hypothesis that USAG-1 functions as a novel BMP-7 antagonist in maxillary supernumerary incisors formation, we analysed adult USAG-$1^{-/-}$/BMP-$7^{+/-}$ mice. The incidence or pattern of supernumerary incisors formation in USAG-$1^{-/-}$/BMP-$7^{+/+}$ and USAG-$1^{-/-}$/BMP-$7^{+/-}$ mice are almost identical, which was about 50% (Table S1). We previously demonstrated that the supernumerary maxillary incisor formed as a result of the successive development of the rudimentary incisor tooth primordia [15]. Therefore, we analysed the maxillary rudiment incisor tooth germ of USAG-$1^{-/-}$/BMP-$7^{-/-}$mice in select embryonic stages. We performed a series of histological investigations of USAG-$1^{+/+}$/BMP-$7^{+/+}$, USAG-$1^{-/-}$/BMP-$7^{+/+}$, USAG-$1^{+/+}$/BMP-$7^{-/-}$ and USAG-$1^{-/-}$/BMP-$7^{-/-}$ mice at E15 and newborn (P0). At E15, the area of the maxillary deciduous incisor was identified in wild type as well as all mutant mice in the labial border of the epithelial invagination (as described by [15,51]). The size of rudimentary incisor is similar except USAG-$1^{+/+}$/BMP-$7^{-/-}$ at E15 (Fig. 2A, A', B, B', C, C', D, D' and I). Rudimentary tooth primordia in USAG-$1^{-/-}$/BMP-$7^{-/-}$ regressed and their size regressed and became smaller at birth. This was also observed for USAG-$1^{+/+}$/BMP-$7^{+/+}$ whereas the tooth organs in USAG-$1^{-/-}$/BMP-$7^{+/+}$ continued to develop and the enamel organ was formed (Fig. 2, E, E', F, F', H, H' and J). USAG-1 abrogation rescued the apoptotic elimination of odontogenic mesenchymal cells in the rudimentary maxillary incisor tooth primordia at E15, whereas the size remained comparable (Fig. 3 A, A', B and B') [15]. The apoptotic mesenchymal cells in USAG-$1^{-/-}$/BMP-$7^{-/-}$are similar to USAG-$1^{+/+}$/BMP-$7^{+/+}$ in contrast to that of USAG-$1^{-/-}$/BMP-$7^{+/+}$ (Fig 3.A, A', B, B', D and D'). These results demonstrate that USAG-1 functions as a BMP-7 antagonist in maxillary supernumerary incisors formation.

Increased BMP signaling in supernumerary teeth of the USAG-1 deficient mice is prohibited by BMP-7 abrogation

To evaluate whether increased BMP signaling in supernumerary teeth of the USAG-1 deficient mice could be prohibited by BMP-7 abrogation, we examined the Msx1 and Dlx2 expression; both of these transcription factors are downstream target genes of BMP-mediated signal transcription during tooth development at E13 [52,53], with complementary phosphorylation of Smad 1/5/8 attributable to increased BMP signaling at E13 [21,54] in USAG-$1^{+/+}$/BMP-$7^{+/+}$, USAG-$1^{-/-}$/BMP-$7^{+/+}$, USAG-$1^{+/+}$/BMP-$7^{-/-}$ and USAG-$1^{-/-}$/BMP-$7^{-/-}$ mice. At E13, Msx1 and Dlx2 expression in the rudimentary maxillary incisors of USAG-$1^{-/-}$/BMP-$7^{-/-}$ mice was comparable with that of USAG-$1^{+/+}$/BMP-$7^{+/+}$, whereas that of USAG-$1^{-/-}$/BMP-$7^{+/+}$ appeared more intense as compared with that in controls (Fig. 4A-H). Further, compared with USAG-$1^{-/-}$/BMP-$7^{+/+}$ embryos, USAG-$1^{-/-}$/BMP-$7^{-/-}$ embryos inhibited increased phosphorylated Smad 1/5/8 based upon positive odontogenic mesenchymal cells within the rudimentary maxillary incisor tooth primordia at E15 (Fig. 5A-D). To determine the specificity of phosphorylation of Smad 1/5/8, we employed immunostaining using anti-phospho-Smad 2/3, and found no difference among mutant mice (Fig. 5E-H). We conclude that increased BMP signaling in supernumerary teeth of the USAG-1 deficient mice is prohibited by BMP-7 abrogation.

BMP-7 induces maxillary supernumerary incisors formation partially but not fully *in vitro*

To test whether BMP-7 actually induces supernumerary tooth formation, we performed explant culture and subsequent subrenal kidney capsule transplantation of E15 USAG-1 mutant maxillary incisor tooth primordia supplemented with BMP-7. We previously showed that the USAG-$1^{+/-}$ mice showed phenotypically normal tooth number and position in maxillary incisor as well as wild type [15]. The incisor explants supplemented with BMP-7 in USAG-

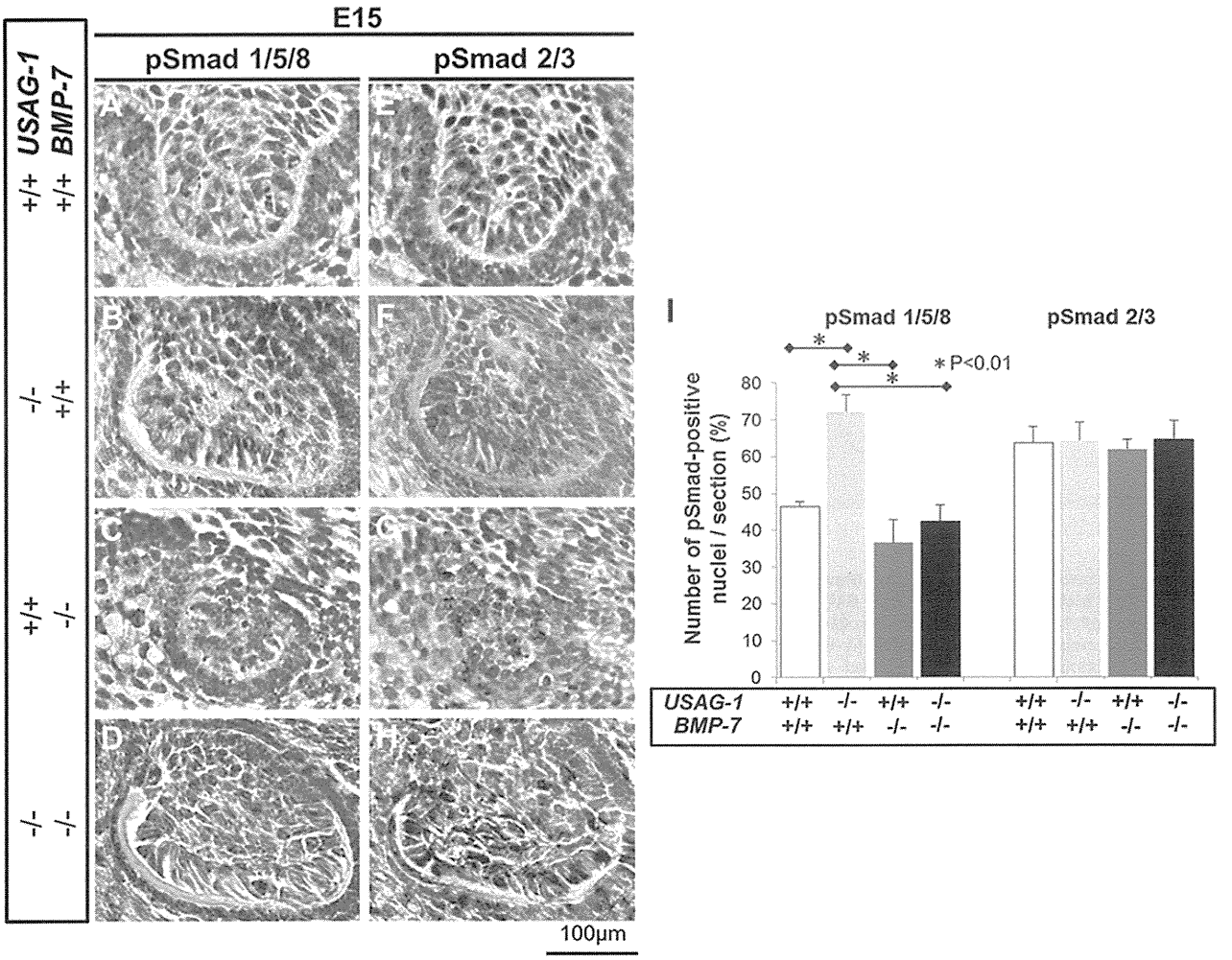

Figure 5. Enhanced BMP signal transduction in maxillary incisors of USAG-1 and BMP-7 mutants. Immunolocalisation of phosphorylated Smad (1/5/8 (A–D) and Smad 2/3 (E–H) at E15. USAG-$1^{+/+}$/BMP-$7^{+/+}$, (A, E); USAG-$1^{-/-}$/BMP-$7^{+/+}$, (B, F); USAG-$1^{+/+}$/BMP-$7^{-/-}$, (C, G) and USAG-$1^{-/-}$/BMP-$7^{-/-}$ (D, H). The number of pSmad 1/5/8– and pSmad 2/3- positive nuclei per section was counted in transverse sections of USAG-$1^{+/+}$/BMP-$7^{+/+}$ (white bars), USAG-$1^{-/-}$/BMP-$7^{+/+}$ (right grey bars), USAG-$1^{+/+}$/BMP-$7^{-/-}$ (dark grey bars), and USAG-$1^{-/-}$/BMP-$7^{-/-}$ (black bars) mice (n = 5; I). Compared with USAG-$1^{-/-}$/BMP-$7^{+/+}$ embryos, USAG-$1^{-/-}$/BMP-$7^{-/-}$ embryos iibited increased phosphorylated Smad 1/5/8- positive cells in odontogenic mesenchymal cells within the rudimentary maxillary incisor primordia at E15 (A–D). Employed immunostaining using anti-phospho-Smad 2/3 showed no difference among mutant mice (E–H). Enhanced BMP signalling in supernumerary teeth of the USAG-1-deficient mice could be inhibited by BMP-7 abrogation.
doi:10.1371/journal.pone.0096938.g005

$1^{+/-}$ as well as USAG-$1^{-/-}$ have supernumerary tooth in similar numbers after 20 days culture, while these cultured explants in USAG-$1^{+/+}$ presented normal tooth number (Fig.6A–J). These results demonstrated BMP-7 has a partial potential to induce supernumerary tooth formation, however it was not readily observed to induce extra tooth organs only with BMP-7.

Discussion

Rudimentary organs are biological structures that appear to have no function as first described by Darwin in The Descent of Man [55]. Darwin listed so-called "wisdom teeth, the appendix, and the coccyx as rudimentary organs. Curiously, Reptiles with teeth as well as most mammals have complete dentitions with Rodentia (mice, rats, hamsters) and Lagomorphs (rabbits) which both present the unique diastema extending from incisor to molar tooth organs in the maxilla as well as mandible. Rather than the diastema truly representing a "toothless" region, a number of studies confirmed that the region in fact does contain rudimental primitive tooth organs at the bud stage of development [56–58]. Tooth organs, comparable to many other epidermal organs, are initiated as a placode and then progress through exquisite epithelial-mesenchymal interactions, reflecting a temporal and spatial sequence of unique signal transduction-mediated developmental processes [2,6,59–64].

In our present study, BMP-7 was co-localized with USAG-1 in the area of the maxillary rudiment incisor tooth germ in addition to the regular maxillary incisor tooth organ. USAG-1 abrogation rescued the apoptotic elimination of mesenchymal cells in the rudimentary maxillary incisor tooth primordia at E15, whereas the tooth sizes were comparable [15]. The apoptotic mesenchymal cells in USAG-$1^{-/-}$/BMP-$7^{-/-}$are similar to USAG-$1^{+/+}$/BMP-$7^{+/+}$ in contrast to that of USAG-$1^{-/-}$/BMP-$7^{+/+}$. These results

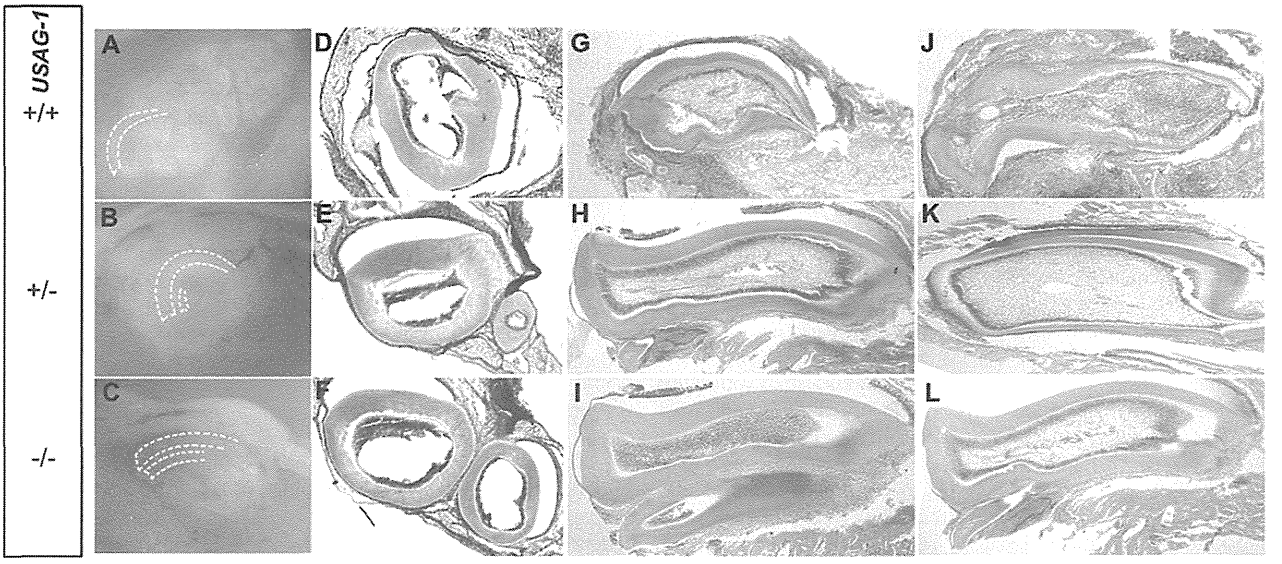

M

USAG-1 Genotype	BMP-7 +		Control	
	Tooth number			
	1	2	1	2
+/+	3/3	0/3	3/3	0/3
+/-	1/4	3/4	3/3	0/3
-/-	1/5 (Fused tooth)	4/5 (2/5 dens in dente)	2/3	1/3

Figure 6. BMP-7 has potential to partially induce the formation of maxillary supernumerary incisors formation in vitro. Enhanced BMP-7 rescue the formation of maxillary incisor supernumerary tooth in E15 USAG-1 mutant mice in organ culture and subrenal capsule assay. The incisor explants supplemented with BMP-7 in USAG-$1^{+/-}$ (E and H) and USAG-$1^{-/-}$ (F and I) have supernumerary tooth in similar incidence after 20 days of culture, whereas these cultured explants in USAG-$1^{+/+}$ (D and G) maintained the normal tooth number. (A–C) Explant appearance. (D–F) Coronal and (G–I) sagittal sections of explant. (J–L) Sagittal sections of control explant. (M) Table showing the relationship between number of teeth of explants and USAG-1 phenotypes.
doi:10.1371/journal.pone.0096938.g006

support our interpretation that USAG-1 functions as a novel BMP-7 antagonist in the maxilla. We confirmed that increased BMP signaling in supernumerary teeth of the USAG-1 deficient mice could be prohibited by BMP-7 abrogation. In the contrast, to test whether BMP-7 has the potential to induce supernumerary tooth formation, we performed explant culture and subsequent subrenal kidney capsule culture. The incisor explants supplemented with BMP-7 in USAG-$1^{+/-}$ as well as USAG-$1^{-/-}$ have supernumerary tooth in similar numbers after 20 days culture, while these cultured explants in USAG-$1^{+/+}$ retained normal tooth number. These results demonstrated that BMP-7 can induce supernumerary tooth formation, however it is impossible to induce extra tooth by only BMP-7. Finally, we conclude that gene interactions between BMP-7 and USAG-1 regulate the supernumerary maxillary incisor formation.

The supernumerary incisors documented in mutant mice have been located on the lingual side of the normal incisor [15,17,23,65], or side-by-side [8,66–69]. The Spry$2^{+/-}$/Spry$4^{-/-}$ mice indicated two separate incisors in two different enamel organs located side by side, in which supernumerary incisor development was shown in vivo to result from the second splitting of the incisor primodium [69]. The duplicated incisors belong to the same generation. Within these supernumerary incisor formation side-by-side, the β-cat$^{\Delta Prx/lacZ}$ mice also present two incisors that each belong to the same generation, but in these mice only the lower incisor have been reported to be affected [68]. The mechanisms of supernumerary formation appear to be different between maxilla and mandibular morphogenesis.

A detailed analysis of USAG-1 deficient mice showed that the supernumerary incisor developed on the lingual side of the normal one, and this tooth was considered to belong to a different tooth generation [15,23]. The supernumerary incisor of Lrp4 deficient mice have the same origin as the supernumerary incisor of USAG-1 mutants [17]. We previously demonstrated that the supernumerary maxillary incisor was the result of the survival and successive development of the rudimentary incisor tooth primordia, and that USAG-1 controls the number of teeth in the maxillary incisor region by regulating apoptotic elimination of odontogenic mesenchymal cells [15].

Further, it was reported that the supernumerary mandibular incisor corresponded to the revival of the replacement incisor by regulating apoptosis of odontogenic epithelial cells [23]. These results suggest that the potential mechanism by which supernumerary incisor on the lingual side of the normal incisor is different between maxilla and mandible. In USAG-1 single deficient mouse, supernumerary teeth were observed in 100% of the maxillary incisor regions, whereas partial penetrance was observed in the mandible. We demonstrated that USAG-1 acted as BMP-7 antagonist in supernumerary maxillary incisor formation, and absence of the maxillary teeth of conditional BMP-7 null mice [44]. The expression of USAG-1 and BMP-7 is opposite around the rudimentary incisor tooth primordia between maxilla and

mandible (Fig. S1). In addition, in mature adult mice, supernumerary teeth can be induced on both labial and lingual sides of the incisors, regions which contain adult stem cells supporting the continuous growth of mouse incisors [22,70]. In young mice, supernumerary tooth organs were induced in multiple regions adjacent to both incisor and molar regions. Presumably, supernumerary tooth organs can form directly from the oral epithelium, in the dental lamina connecting the developing molar or incisor tooth organs to the oral epithelium, in the crown region, and even in the elongating and furcation area of the developing root [22].

In the rudimentary maxillary incisor of BMP-7 deficient mouse, specific phenotypic alterations are found. In approximately half of the embryos studied, the rudimentary maxillary incisors were discovered to be missing. Defects in odontogenesis have been reported in several mouse mutants for genes associated with BMP as well as other signaling pathways [3,71]. Deletion of Alk3 (BMPR1a) in the epithelium leads to tooth development arrest at the bud stage [72], indicating the importance of mesenchyme-derived BMP signals for the further development of the dental epithelium. The epithelial overexpression of Noggin, which is an antagonist of the BMP signaling, results in various phenotypic alterations including lack of mandibular molars, reduced number of maxillary molars, disrupted root size and pattern, as well as poorly mineralized enamel [73]. In Msx1-deficient mice tooth development is arrested at the cup stage [74], a phenotype that can be rescued by administration of BMP-4 [75]. In vitro, BMP-4 and BMP-7 can both induce the expression of Msx1 and Msx2 as shown by the implantation of BMP-releasing beads into the mouse molar mesenchyme [52,76]. The present report provides the direct functional evidence of a nonredundant role for BMPs in tooth initiation and development. The fact that the observed phenotypes are not fully penetrant could be explained by a partial redundancy where other BMPs or other signaling molecules compensate for BMP-7. As BMPs show different affinities for the various type I BMP receptors, a molecular discrimination between signals initiated by different BMPs under physiological conditions is expected. An indication of the importance of BMP-7 for aspects as variable as tooth induction, patterning, and development comes from observations showing different degree of phenotype penetrance in incisors vs. molars as well as in maxillary teeth vs. mandibular teeth. The molecular networks that determine rodent tooth specification (i.e. molars and incisors, maxillary and mandibular teeth) involve genes such as the Islet1, Pitx1, Barx1, and Dlx [77–79], thus integrating BMP-7 into their pathway.

The presence of epithelial anlagen of the third dentition was also noticed in human [80–82]. The epithelium which is considered as the anlagen of the third dentition develops lingual to all permanent tooth germs [83]. Furthermore, when it appears, the predecessor (permanent tooth germ) is in the bell-shaped stage [83]. The time of appearance of the third dentition seems after birth. This means that we have chance to access the formation of the third dentition in the mouth. Recently, a number of mouse mutant are now starting to provide some insights into the mechanisms of supernumerary tooth formation. Multiple supernumerary teeth may have genetic components in their etiology and represent partial of the third dentition in humans. Such candidate molecules or genes might be those that are involved in embryonic tooth induction, in successional tooth formation or in the control of the number of the teeth [2].

The supernumerary tooth formation using genetically-defined mouse models clearly demonstrate the feasibility to induce de novo tooth formation by in situ repression or activation of a single candidate gene. Our investigations and related support or validate the hypothesis that de novo repression or activation of candidate genes such as BMP-7 or USAG-1 could be used to stimulate a third dentition to induce or achieve new tooth regeneration in mammals. In vivo gene delivery could be the suitable gene therapy approach in the tooth regeneration by stimulation of a third dentition.

Conclusions

The mechanism for suppressing deciduous incisors in mice is expression of USAG-1, which inhibits BMP-7 signaling, leading to apoptosis and degeneration of rudimentary tooth germs. The dental phenotypes of USAG-1 and BMP-7 mutants reported by our studies provide a rationale for future tooth regeneration.

Supporting Information

Figure S1 The expression of USAG-1 and BMP-7 in the lower jaws. USAG-1 and BMP-7 expression in mandibular incisor primordia. (A–D) Whole-mount X-Gal expression in tooth germs of E14 and E15 mandibular. (A'–D') Parasagittal sections (anterior to the left) of the tooth germs. USAG-1 (A–B, A'–B') and BMP-7 (C–D, C'–D') were expressed in the tooth organ of rudimentary mandibular incisor (red arrow) in addition to the tooth organ of characteristic incisor (black arrow). At E14, USAG-1 started to be expressed in the epithelial cells of the mandibular rudimentary and regular incisor primordia (A and A'). At E15, the expression of USAG-1 continued in the epithelium (B and B'). In the meantime, the expression of BMP-7 localized mesenchymal cells of mandibular rudimentary and regular incisor primordia at both E14 and E15 (C, D, C' and D').
(TIF)

Table S1 Summary of tooth phenotype.
(DOCX)

Acknowledgments

The paper is indebted to Dr. Motoko Yanagita for helpful discussion. BMP-7 KO mice is kindly gift from Dr. Elizabeth Robertson in University of Oxford.

Author Contributions

Conceived and designed the experiments: HK KT MS AS Y. Tabata HS KB. Performed the experiments: HK KS Y. Togo HT BH. Analyzed the data: HK KT KS Y. Togo HT KB. Contributed reagents/materials/analysis tools: MS KT AS Y. Tabata AE. Wrote the paper: HK KT BH HS.

References

1. Epstein CJ, Erickson RP, Wynshaw-Boris AJ (2008) Inborn errors of development: the molecular basis of clinical disorders of morphogenesis. Second edition. Oxford: Oxford University Press.
2. Ohazama A, Sharpe PT (2008) Development of epidermal appendages: Teeth and Hair. In: Epstein CJ, Erickson RP, Wynshaw-Boris A, editors. Inborn errors of development: the molecular basis of clinical disorders of morphogenesis. Second edition. Oxford: Oxford University Press. pp. 245–262.
3. Brown A, Stock G, Patel AA, Okafor C, Vaccaro A (2006) Osteogenic protein-1: a review of its utility in spinal applications. BioDrugs: clinical immunotherapeutics, biopharmaceuticals, and gene therapy 20: 243–251.
4. Schulze C (1970) Developmental abnormalities of the teeth and jaws. Thoma's oral pathology 1: 112–122.
5. Yusof WZ (1990) Non-syndrome multiple supernumerary teeth: literature review. J Can Dent Assoc 56: 147–149.

6. Slavkin HC (2012) The Birth of a Discipline: Craniofacial Biology. Newton, PA: Aegis Communications.
7. Zhou P, Byrne C, Jacobs J, Fuchs E (1995) Lymphoid enhancer factor 1 directs hair follicle patterning and epithelial cell fate. Genes Dev 9: 700–713.
8. Kaufman MH, Chang HH, Shaw JP, (1995) Craniofacial abnormalities in homozygous Small eye (Sey/Sey) embryos and newborn mice. Journal of anatomy 186: 607–617.
9. Mustonen T, Pispa J, Mikkola ML, Pummila M, Kangas AT, et al. (2003) Stimulation of ectodermal organ development by Ectodysplasin-A1. Developmental biology 259: 123–136.
10. Zhang Q, Murcia NS, Chittenden LR, Richards WG, Michaud EJ, et al. (2003) Loss of the Tg737 protein results in skeletal patterning defects. Developmental dynamics 227: 78–90.
11. Pispa J, Mustonen T, Mikkola ML, Kangas AT, Koppinen P, et al. (2004) Tooth patterning and enamel formation can be manipulated by misexpression of TNF receptor Edar. Developmental dynamics 231: 432–440.
12. Tucker AS, Headon DJ, Courtney JM, Overbeek P, Sharpe PT (2004) The activation level of the TNF family receptor, Edar, determines cusp number and tooth number during tooth development. Developmental biology 268: 185–194.
13. Klein OD, Minowada G, Peterkova R, Kangas A, Yu BD, et al. (2006) Sprouty genes control diastema tooth development via bidirectional antagonism of epithelial-mesenchymal FGF signaling. Developmental cell 11: 181.
14. Järvinen E, Salazar-Ciudad I, Birchmeier W, Taketo MM, Jernvall J, et al. (2006) Continuous tooth generation in mouse is induced by activated epithelial Wnt/beta-catenin signaling. Proceedings of the National Academy of Sciences - PNAS 103: 18627–18632.
15. Murashima-Suginami A, Takahashi K, Kawabata T, Sakata T, Tsukamoto H, et al. (2007) Rudiment incisors survive and erupt as supernumerary teeth as a result of USAG-1 abrogation. Biochemical and biophysical research communications 359: 549–555.
16. Nakamura T, deVega S, Fukumoto S, Jimenez L, Unda F, et al. (2008) Transcription factor epiprofin is essential for tooth morphogenesis by regulating epithelial cell fate and tooth number. The Journal of biological chemistry 283: 4825–4833.
17. Ohazama A, Johnson EB, Ota MS, Choi HY, Porntaveetus T, et al. (2008) Lrp4 modulates extracellular integration of cell signaling pathways in development. PloS one 3: e4092.
18. Zhang Z, Lan Y, Chai Y, Jiang R (2009) Antagonistic actions of Msx1 and Osr2 pattern mammalian teeth into a single row. Science 323: 1232–1234.
19. Huang B, Takahashi K, Sakata-Goto T, Kiso H, Togo Y, et al. (2013) Phenotypes of CCAAT/enhancer-binding protein beta deficiency: hyperdontia and elongated coronoid process. Oral diseases 19: 144–150.
20. Takahashi K, Kiso H, Saito K, Togo Y, Tsukamoto H, et al. (2013) Feasibility of gene therapy for tooth regeneration by stimulation of a third dentition: Gene Therapy - Tools and Potential Applications. DOI: 10.5772/52529.
21. Murashima-Suginami A, Takahashi K, Sakata T, Tsukamoto H, Sugai M, et al. (2008) Enhanced BMP signaling results in supernumerary tooth formation in USAG-1 deficient mouse. Biochemical and biophysical research communications 369: 1012–1016.
22. Wang XP, O'Connell DJ, Lund JJ, Saadi I, Kuraguchi M, et al. (2009) Apc inhibition of Wnt signaling regulates supernumerary tooth formation during embryogenesis and throughout adulthood. Development 136: 1939–1949.
23. Munne PM, Tummers M, Järvinen E, Thesleff I, Jernvall J (2009) Tinkering with the inductive mesenchyme: Sostdc1 uncovers the role of dental mesenchyme in limiting tooth induction. Development 136: 393–402.
24. Munne PM, Felszeghy S, Jussila M, Suomalainen M, Thesleff I, et al. (2010) Splitting placodes: effects of bone morphogenetic protein and Activin on the patterning and identity of mouse incisors. Evolution & development 12: 383–392.
25. Hovorakova M, Prochazka J, Lesot H, Smrckova L, Churava S, et al. (2011) Shh expression in a rudimentary tooth offers new insights into development of the mouse incisor. Journal of experimental zoology Part B, Molecular and developmental evolution 316: 347–358.
26. Lagronova-Churava S, Spoutil F, Vojtechova S, Lesot H, Peterka M, et al. (2013) The dynamics of supernumerary tooth development are differentially regulated by Sprouty genes. Journal of experimental zoology Part B, Molecular and developmental evolution 320: 307–320.
27. Yamamoto H, Cho SW, Song SJ, Hwang HJ, Lee MJ, et al. (2005) Characteristic tissue interaction of the diastema region in mice. Archives of oral biology 50: 189–198.
28. Peterková R, Lesot H, Viriot L, Peterka M (2005) The supernumerary cheek tooth in tabby/EDA mice-a reminiscence of the premolar in mouse ancestors. Archives of oral biology 50: 219–225.
29. Prochazka J, Pantalacci S, Churava S, Rothova M, Lambert A, et al. (2010) Patterning by heritage in mouse molar row development. Proceedings of the National Academy of Sciences - PNAS 107: 15497–15502.
30. Ohazama A, Haycraft CJ, Seppala M, Blackburn J, Ghafoor S, et al. (2009) Primary cilia regulate Shh activity in the control of molar tooth number. Development 136: 897–903.
31. Yanagita M, Oka M, Watabe T, Iguchi H, Niida A, et al. (2004) USAG-1: a bone morphogenetic protein antagonist abundantly expressed in the kidney. Biochemical and biophysical research communications 316: 490–500.
32. Yanagita M (2005) BMP antagonists: their roles in development and involvement in pathophysiology. Cytokine & growth factor reviews 16: 309–317.
33. Graham A, Koentges G, Lumsden A (1996) Neural crest apoptosis and the establishment of craniofacial pattern: an honorable death. Molecular and cellular neurosciences 8: 76–83.
34. Zuzarte-Luis V, Hurle JM (2005) Programmed cell death in the embryonic vertebrate limb. Seminars in cell & developmental biology 16: 261–269.
35. Gañan Y, Macias D, Duterque-Coquillaud M, Ros MA, Hurle JM (1996) Role of TGF beta s and BMPs as signals controlling the position of the digits and the areas of interdigital cell death in the developing chick limb autopod. Development 122: 2349–2357.
36. Graham A, Francis-West P, Bickell P, Lumsden A (1994) The signalling molecule BMP4 mediates apoptosis in the rhombencephalic neural crest. Nature 372: 684–686.
37. Takahashi K, Nuckolls GH, Tanaka O, Semba I, Takahashi I, et al. (1998) Adenovirus-mediated ectopic expression of Msx2 in even-numbered rhombomeres induces apoptotic elimination of cranial neural crest cells in ovo. Development 125: 1627–1635.
38. Luo G, Hofmann C, Bronckers AL, Sohocki M, Bradley A, et al. (1995) BMP-7 is an inducer of nephrogenesis, and is also required for eye development and skeletal patterning. Genes & development 9: 2808–2820.
39. Li T, Surendran K, Zawaideh MA, Mathew S, Hruska KA (2004) Bone morphogenetic protein 7: a novel treatment for chronic renal and bone disease. Current opinion in nephrology and hypertension 13: 417–422.
40. Miyazaki Y, Oshima K, Fogo A, Ichikawa I (2003) Evidence that bone morphogenetic protein 4 has multiple biological functions during kidney and urinary tract development. Kidney international 63: 835–844.
41. Yanagita M, Okuda T, Endo S, Tanaka M, Takahashi K, et al. (2006) Uterine sensitization-associated gene-1 (USAG-1), a novel BMP antagonist expressed in the kidney, accelerates tubular injury. The Journal of clinical investigation 116: 70–79.
42. Dudley AT, Lyons KM, Robertson EJ (1995) A requirement for bone morphogenetic protein-7 during development of the mammalian kidney and eye. Genes & development 9: 2795–2807.
43. Wawersik S, Purcell P, Rauchman M, Dudley AT, Robertson EJ, et al. (1999) BMP7 acts in murine lens placode development. Developmental biology 207: 176–188.
44. Zouvelou V, Luder HU, Mitsiadis TA, Graf D (2009) Deletion of BMP7 affects the development of bones, teeth, and other ectodermal appendages of the orofacial complex. Journal of experimental zoology Part B, Molecular and developmental evolution 312B: 361–374.
45. Tanaka M, Endo S, Okuda T, Economides AN, Valenzuela DM, et al. (2008) Expression of BMP-7 and USAG-1 (a BMP antagonist) in kidney development and injury. Kidney international 73: 181–191.
46. Godin RE, Takaesu NT, Robertson EJ, Dudley AT (1998) Regulation of BMP7 expression during kidney development. Development 125: 3473–3482.
47. Nadiri A, Kuchler-Bopp S, Haikel Y, Lesot H (2004) Immunolocalization of BMP-2/-4, FGF-4, and WNT10b in the developing mouse first lower molar. The journal of histochemistry and cytochemistry 52: 103–112.
48. Aoki K, Tamai Y, Horiike S, Oshima M, Taketo MM, et al. (2003) Colonic polyposis caused by mTOR-mediated chromosomal instability in Apc/Delta716 Cdx2/- compound mutant mice. Nature genetics 35: 323–330.
49. Ikada Y, Tabata Y (1998) Protein release from gelatin matrices. Advanced drug delivery reviews 31: 287–301.
50. Tabata Y, Ikeda Y (1999) Vascularization effect of basic fibroblast growth factor released from gelatin hydrogels with different biodegradabilities. Biomaterials 20: 2169–2175.
51. Fitzgerald LR (1973) Deciduous incisor teeth of the mouse (Mus musculus). Archives of oral biology 18: 381–389.
52. Vainio S, Karavanova I, Jowett A, Thesleff I (1993) Identification of BMP-4 as a signal mediating secondary induction between epithelial and mesenchymal tissues during early tooth development. Cell 75: 45–58.
53. Thomas BL, Liu JK, Rubenstein JL, Sharpe PT (2000) Independent regulation of Dlx2 expression in the epithelium and mesenchyme of the first branchial arch. Development 127: 217–224.
54. Sakata-Goto T, Takahashi K, Kiso H, Huang B, Tsukamoto H, et al. (2012) Id2 controls chondrogenesis acting downstream of BMP signaling during maxillary morphogenesis. Bone 50: 69–78.
55. Darwin CR (1871) The Descent of Man, and Selection in Relation to Sex. London: John Murray.
56. Keränen SV, Kettunen P, Åberg T, Thesleff I, Jernvall J (1999) Gene expression patterns associated with suppression of odontogenesis in mouse and vole diastema regions. Development genes and evolution 209: 495–506.
57. Peterková R, Peterka M, Viriot L, Lesot H (2000) Dentition development and budding morphogenesis. Journal of craniofacial genetics and developmental biology 20: 158–172.
58. Peterková R, Peterka M, Viriot L, Lesot H (2002) Development of the vestigial tooth primordia as part of mouse odontogenesis. Connective tissue research 43: 120–128.
59. Slavkin HC (1972) Intercellular communication during odontogenesis. In: Slavkin HC, Bavetta LA, editors. Developmental aspects of oral biology. New York: Academic Press Inc. pp165–197.
60. Slavkin HC (1979) Developmental craniofacial biology. Philadelphia: Lea and Febiger.
61. Kollar EJ (1972) Histogenetic aspects of dermal-epidermal interactions. Developmental aspects of oral biology: 125–149.

62. Kollar EJ (1972) The Development of the Integument Spatial, Temporal, and Phylogenetic Factors. American Zoologist 12: 125–135.
63. Maas R, Bei M (1997) The genetic control of early tooth development. Critical reviews in oral biology and medicine 8: 4–39.
64. Thesleff I, Vaahtokari A, Vainio S, Jowett A (1996) Molecular mechanisms of cell and tissue interactions during early tooth dvelopment. The Anatomical record 245: 151–161.
65. Danforth CH (1958) The Occurrence and Genetic Behavior of Duplicate Lower Incisors in the Mouse. Genetics 43: 139–148.
66. Sofaer JA (1969) Aspects of the tabby-crinkled-downless syndrome. I. The development of tabby teeth. Journal of embryology and experimental morphology 22: 181–205.
67. Klopcic B, Maass T, Meyer E, Lehr HA, Metzger D, et al. (2007) TGF-beta superfamily signaling is essential for tooth and hair morphogenesis and differentiation. European journal of cell biology 86: 781–799.
68. Fujimori S, Novak H, Weissenböck M, Jussila M, Gonçalves A, et al. (2010) Wnt/β-catenin signaling in the dental mesenchyme regulates incisor development by regulating Bmp4. Developmental biology 348: 97–106.
69. Charles C, Hovorakova M, Ahn Y, Lyons DB, Marangoni P, et al. (2011) Regulation of tooth number by fine-tuning levels of receptor-tyrosine kinase signaling. Development 138: 4063–4073.
70. Liu F, Dangaria S, Andl T, Zhang Y, Wright AC, et al. (2010) beta-Catenin initiates tooth neogenesis in adult rodent incisors. Journal of dental research 89: 909–914.
71. Schneider M, Hansen JL, Sheikh SP (2008) S100A4: a common mediator of epithelial-mesenchymal transition, fibrosis and regeneration in diseases? Journal of molecular medicine 86: 507–522.
72. Andl T, Ahn K, Kairo A, Chu EY, Wine-Lee L, et al. (2004) Epithelial Bmpr1a regulates differentiation and proliferation in postnatal hair follicles and is essential for tooth development. Development 131: 2257–2268.
73. Plikus MV, Zeichner-David M, Mayer JA, Reyna J, Bringas P, et al. (2005) Morphoregulation of teeth: modulating the number, size, shape and differentiation by tuning Bmp activity. Evolution & development 7: 440–457.
74. Satokata I, Mass R (1994) Msx1 deficient mice exhibit cleft palate and abnormalities of craniofacial and tooth development. Nature genetics 6: 348–356.
75. Bei M, Kratochwil K, Maas R (2000) BMP4 rescues a non-cell-autonomous function of Msx1 in tooth development. Development 127: 4711–4718.
76. Wang YH, Rutherford B, Upholt WB, Mina M, (1999) Effects of BMP-7 on mouse tooth mesenchyme and chick mandibular mesenchyme. Developmental dynamics 216: 320–335.
77. Thomas BL, Tucker AS, Qui M, Ferguson CA, Hardcastle Z, et al. (1997) Role of Dlx-1 and Dlx-2 genes in patterning of the murine dentition. Development 124: 4811–4818.
78. Mitsiadis TA, Angeli I, James C, Lendahl U, Sharpe PT (2003) Role of Islet1 in the patterning of murine dentition. Development 130: 4451–4460.
79. Mitsiadis TA, Drouin J (2008) Deletion of the Pitx1 genomic locus affects mandibular tooth morphogenesis and expression of the Barx1 and Tbx1 genes. Developmental biology 313: 887–896.
80. Röse C (1895) Überreste einer vorzeitigen prälactealen und einer vierten Zahnreihe beim Menschen. Österreichisch-ungarische Vierteljahrschr Zahnheilk 2: 45–50.
81. Ahrens H (1913) Die Entwickelung der Menschlichen Zähne. Anatomische Hefte 48: 167–266.
82. Fujita K (1958) Abnormality of teeth number in human. J Stomatol Soc Jpn 25: 97–106.
83. Ooë T (1969) Epithelial anlagen of human third dentition and their migrations in the mandible and maxilla. Okajimas folia anatomica japonica 46: 243–251.

Endocrine Journal 2014, **61** (7), 735-742

NOTE

Clinical effects of ghrelin on gastrointestinal involvement in patients with systemic sclerosis

Hiroyuki Ariyasu[1), 2), 9)], Hiroshi Iwakura[1), 2)], Naoichiro Yukawa[3)], Toshinori Murayama[4)], Masayuki Yokode[4)], Harue Tada[5)], Kenichi Yoshimura[5)], Satoshi Teramukai[5)], Tatsuya Ito[6)], Akira Shimizu[6)], Atsushi Yonezawa[7)], Kenji Kangawa[8)], Tsuneyo Mimori[3)] and Takashi Akamizu[1), 9)]

[1)] *Ghrelin Research Project, Translational Research Center, Kyoto University Hospital, Kyoto 606-8507, Japan*
[2)] *Department of Endocrinology and Metabolism, Graduate School of Medicine Kyoto University, Kyoto 606-8507, Japan*
[3)] *Department of Rheumatology and Clinical Immunology, Graduate School of Medicine, Kyoto University, Kyoto 606-8507, Japan*
[4)] *Department of Clinical Innovative Medicine, Translational Research Center, Kyoto University Hospital, Kyoto 606-8507, Japan*
[5)] *Department of Clinical Trial Design and Management, Translational Research Center, Kyoto University Hospital, Kyoto 606-8507, Japan*
[6)] *Department of Experimental Therapeutics, Translational Research Center, Kyoto University Hospital, Kyoto 606-8507, Japan*
[7)] *Department of Pharmacy, Kyoto University Hospital, Kyoto 606-8507, Japan*
[8)] *National Cerebral and Cardiovascular Center Research Institute, Osaka 565-8565, Japan*
[9)] *The 1st Department of Internal Medicine, Wakayama Medical University, Wakayama 641-8509, Japan*

Abstract. The majority of patients with systemic sclerosis (SSc) have gastrointestinal (GI) tract involvement, but therapies using prokinetic agents are usually unsatisfactory. Ghrelin stimulates gastric motility in healthy human volunteers. In this study, we investigated whether ghrelin could improve gastric emptying in patients with gastrointestinal symptoms due to SSc. The study was performed in a randomized, double-blind, placebo-controlled crossover fashion on two occasions. Ten SSc patients with GI tract involvement received an infusion of either ghrelin (5.0 μg/kg) or saline, and gastric emptying rate was evaluated by ^{13}C-acetic acid breath test. Gastric emptying was significantly accelerated by ghrelin infusion in patients with SSc (ghrelin *vs.* saline: 43.3 ± 11.4 min *vs.* 53.4 ± 5.4 min, P=0.03). No serious adverse effects were observed. Our results suggest that ghrelin might represent a new therapeutic approach for GI tract involvement in patients with SSc.

Key words: Gastric motility, Ghrelin, Systemic sclerosis

SYSTEMIC SCLEROSIS (SSc) is a progressive and multisystem disease characterized by microvascular damage and excess deposition of connective tissue in skin and internal organs, including kidneys, heart, lungs, and gastrointestinal tract. Therefore, patients with SSc have various symptoms such as Raynaud's phenomenon, thickened or hardened skin, and scleroderma renal crisis. In addition to these symptoms, any part of the gastrointestinal (GI) tract can be affected in patients with SSc, and they often have dysphagia, heartburn, bloating, abdominal pain, and diarrhea [1, 2]. Although involvement of the GI tract is not a direct cause of death, it leads to a decline in the quality of life. In an autopsy study, GI muscle atrophy and fibrosis (both of which lead to decreased GI motility) were detected in the esophagus, small intestine, and colon in 74%, 48%, and 39% of patients, respectively [3]. In previous studies, 50–67% of patients with SSc report delayed gastric emptying, which correlates with symptoms of early satiety, bloating, and emesis [4-12]. At present, the cause of scleroderma is still unknown, and there are no effective treatments for SSc. Consequently, the various complications of SSc are treated individually. To treat gastroparesis, prokinetic agents such as metoclopramide, domperidone, erythromycin, mosapride citrate, dinoprost, and octreotide have been used in an attempt to improve GI motility; however, therapies with these agents are usually unsatisfactory [13-17].

Ghrelin, a gut hormone that is produced mainly in the stomach, is a 28–amino acid peptide with an n-oc-

Submitted Feb. 27, 2014; Accepted Mar. 25, 2014 as EJ14-0088
Released online in J-STAGE as advance publication Apr. 17, 2014
Correspondence to: Hiroyuki Ariyasu, The 1st Department of Internal Medicine, Wakayama Medical University, 811-1 Kimiidera, Wakayama 641-8509, Japan. E-mail: ariyasu@wakayama-med.ac.jp